

Unsymmetrical Platinum(II) Phosphido Derivatives: Oxidation and Reductive Coupling Processes Involving Platinum(III) Complexes as Intermediates[†]

Irene Ara,[‡] Juan Forniés,^{*‡} Consuelo Fortuño,^{*‡} Susana Ibáñez,[‡] Antonio Martín,[‡] Piero Mastrolilli,[§] and Vito Gallo[§]

Departamento de Química Inorgánica and Instituto de Ciencia de Materiales de Aragón, Universidad de Zaragoza, CSIC, 50009 Zaragoza, Spain, and Dipartimento di Ingegneria delle Acque e di Chimica del Politecnico di Bari, via Orabona 4, I-70125 Bari, Italy

Received June 16, 2008

Reaction of the trinuclear $[\text{NBu}_4]_2[(\text{R}_F)_2\text{Pt}(\mu\text{-PPh}_2)_2\text{Pt}(\mu\text{-PPh}_2)_2\text{Pt}(\text{R}_F)_2]$ (**1**, $\text{R}_F = \text{C}_6\text{F}_5$) with HCl results in the formation of the unusual anionic hexanuclear derivative $[\text{NBu}_4]_2\{[(\text{R}_F)_2\text{Pt}(\mu\text{-PPh}_2)_2\text{Pt}(\mu\text{-PPh}_2)_2\text{Pt}(\mu\text{-Cl})]_2\}$ (**4**, 96 e⁻ skeleton) through the cleavage of two Pt–C₆F₅ bonds. The reaction of **4** with Tl(acac) yields the trinuclear $[\text{NBu}_4][(\text{R}_F)_2\text{Pt}(\mu\text{-PPh}_2)_2\text{Pt}(\mu\text{-PPh}_2)_2\text{Pt}(\text{acac})]$ (**5**, 48 e⁻ skeleton), which is oxidized by Ag⁺ to form the trinuclear compound $[(\text{R}_F)_2\text{Pt}(\mu\text{-PPh}_2)_2\text{Pt}(\mu\text{-PPh}_2)_2\text{Pt}(\text{acac})][\text{ClO}_4]$ (**6**, 46 e⁻ skeleton) in mixed oxidation state Pt(III)–Pt(III)–Pt(II), which displays a Pt–Pt bond. The reduction of **6** by $[\text{NBu}_4][\text{BH}_4]$ gives back **5**. The treatment of **6** with Br⁻ (1:1 molar ratio) at room temperature gives a mixture of the isomers $[(\text{PPh}_2\text{R}_F)(\text{R}_F)\text{Pt}(\mu\text{-PPh}_2)(\mu\text{-Br})\text{Pt}(\mu\text{-PPh}_2)_2\text{Pt}(\text{acac})]$, having Br trans to R_F (**7a**) or Br cis to R_F (**7b**), which are the result of PPh₂/C₆F₅ reductive coupling. The treatment of **5** with I₂ (1:1 molar ratio) yields the hexanuclear $\{[(\text{PPh}_2\text{R}_F)(\text{R}_F)\text{Pt}(\mu\text{-PPh}_2)(\mu\text{-I})\text{Pt}(\mu\text{-PPh}_2)_2\text{Pt}(\mu\text{-I})]_2\}$ (**8**, 96 e⁻ skeleton), which is easily transformed into the trinuclear compound $[(\text{PPh}_2\text{R}_F)(\text{R}_F)\text{Pt}(\mu\text{-PPh}_2)(\mu\text{-I})\text{Pt}(\mu\text{-PPh}_2)_2\text{Pt}(\text{I})(\text{PPh}_3)]$ (**9**, 48 e⁻ skeleton). Reaction of $[(\text{R}_F)_2\text{Pt}(\mu\text{-PPh}_2)_2\text{Pt}(\mu\text{-PPh}_2)_2\text{Pt}(\text{NCMe})_2]$ (**10**) with I₂ at 213 K for short reaction times gives the trinuclear platinum derivative $[(\text{R}_F)_2\text{Pt}(\mu\text{-PPh}_2)_2\text{Pt}(\mu\text{-PPh}_2)_2\text{Pt}(\text{I})_2]$ (**11**, 46e skeleton) in mixed oxidation state Pt(III)–Pt(III)–Pt(II) and with a Pt–Pt bond, while the reaction at room temperature and longer reactions times gives **8**. The structures of the complexes have been established by multinuclear NMR spectroscopy. In particular, the ¹⁹⁵Pt NMR analysis, carried out also by ¹⁹F–¹⁹⁵Pt heteronuclear multiple-quantum coherence, revealed an unprecedented shielding of the ¹⁹⁵Pt nuclei upon passing from Pt(II) to Pt(III). The X-ray diffraction structures of complexes **4**, **5**, **6**, **9**, and **11** have been studied. A detailed study of the relationship between the complexes has been carried out.

Introduction

The binuclear platinate(II) derivatives with diphenylphosphido groups as bridging ligands $[(\text{R}_F)_2\text{Pt}(\mu\text{-PPh}_2)_2\text{PtL}_2]^{n-}$ ($\text{R}_F = \text{C}_6\text{F}_5$; $\text{L} = \text{R}_F$, $n = 2$; $\text{L}_2 = \text{acac}$, $n = 1$) react with AgClO₄, affording the binuclear platinum(III) $[(\text{R}_F)_2\text{Pt}(\mu\text{-PPh}_2)_2\text{Pt}(\text{R}_F)_2]$ ¹ or the hexanuclear $[\{\text{AgPt}_2(\mu\text{-PPh}_2)_2(\text{R}_F)_2-$

$(\text{acac})_2\}_2]$ derivatives, which show a Pt(III)–Pt(III) bond or donor/acceptor Pt(II)–Ag(I) bonds, respectively. The replacement of an acac chelate ligand for two terminal pentafluorophenyl groups generates important differences in their reactivity. We have reported that the symmetric trinuclear platinate(II) derivative $[\text{NBu}_4]_2[(\text{R}_F)_2\text{Pt}(\mu\text{-PPh}_2)_2\text{Pt}(\mu\text{-PPh}_2)_2\text{Pt}(\text{R}_F)_2]$ (**1**), with only pentafluorophenyl groups as terminal ligands, is oxidized to the neutral derivative $[(\text{R}_F)_2\text{Pt}(\mu\text{-PPh}_2)_2\text{Pt}(\mu\text{-PPh}_2)_2\text{Pt}(\text{R}_F)_2]$ ³ (**2**), with formally two

* Authors to whom correspondence should be addressed. Fax: +349767-61187 (J.F.). E-mail: juan.fornies@unizar.es (J.F.); cfortuno@unizar.es (C.F.)

[†] Polynuclear Homo- or Heterometallic Palladium(II)–Platinum(II) Pentafluorophenyl Complexes Containing Bridging Diphenylphosphido Ligands. 25. For part 24, see ref 58.

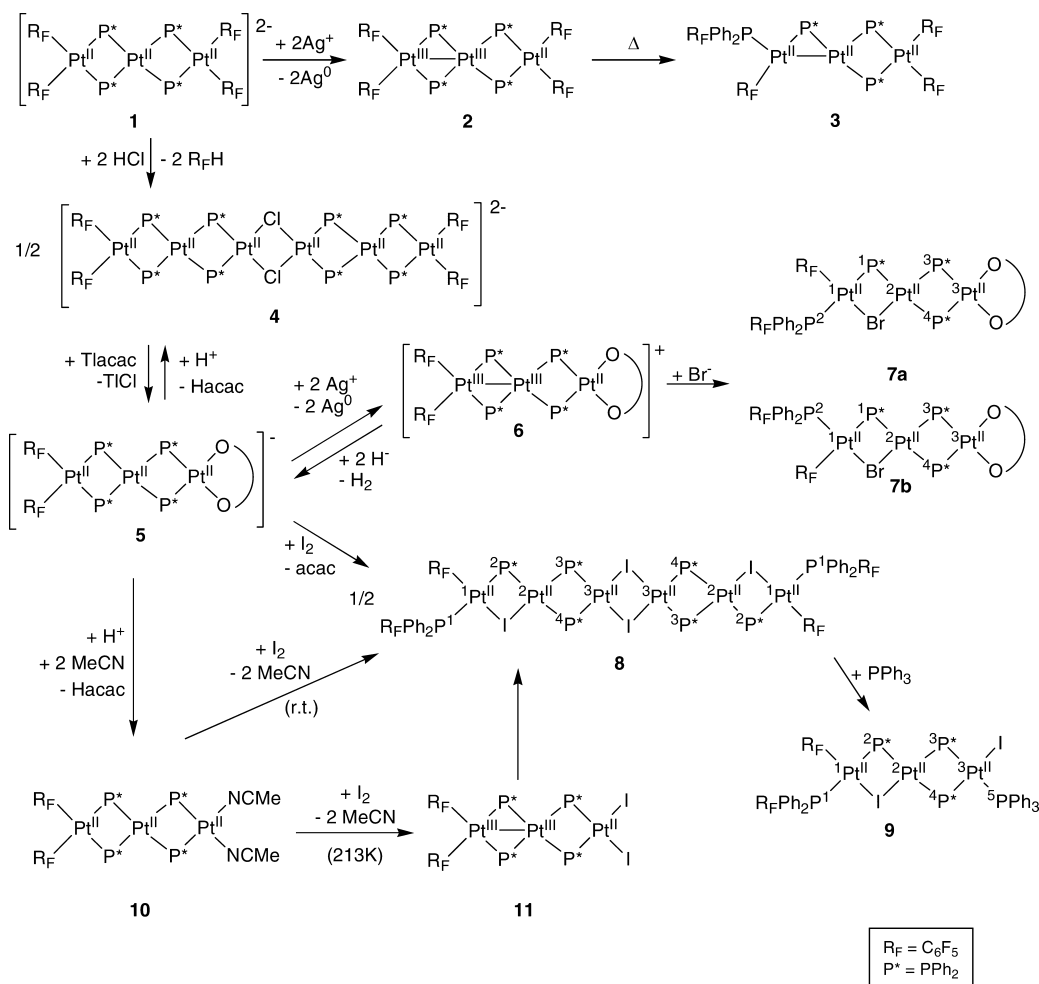
[‡] Dipartimento di Ingegneria delle Acque e di Chimica del Politecnico di Bari.

[§] Universidad de Zaragoza.

(1) Alonso, E.; Casas, J. M.; Cotton, F. A.; Feng, X. J.; Forniés, J.; Fortuño, C.; Tomás, M. *Inorg. Chem.* **1999**, *38*, 5034–5040.

(2) Alonso, E.; Forniés, J.; Fortuño, C.; Martín, A.; Orpen, A. G. *Organometallics* **2003**, *22*, 5011–5019.

Scheme 1



platinum(III) centers, and which evolves to the platinum(II) derivative $[(\text{PPh}_2\text{R}_F)(\text{R}_F)\text{Pt}(\mu\text{-PPh}_2)_2\text{Pt}(\mu\text{-PPh}_2)_2\text{Pt}(\text{R}_F)_2]^{4-}$ (**3**, Scheme 1).

With the aim of obtaining information on the influence of terminal ligands on the behavior of the metal centers within these phosphido derivatives, we have now studied the reactivity of the *unsymmetrical* platinum(II) derivatives $[(\text{R}_F)_2\text{Pt}(\mu\text{-PPh}_2)_2\text{Pt}(\mu\text{-PPh}_2)_2\text{Pt}(\text{L}_2)]^{n-}$. In this type of complex, the three different metal centers are potential Lewis bases, able to establish donor–acceptor Pt–Ag bonds. The oxidation of the platinum complexes, that is, the formation of a derivative with a Pt(III)–Pt(III) bond, which can be established between the central platinum atom and one of the two terminal metallic centers, cannot be discarded. In this paper, we describe the synthetic strategy used to isolate the new *unsymmetrical* $[(\text{R}_F)_2\text{Pt}(\mu\text{-PPh}_2)_2\text{Pt}(\mu\text{-PPh}_2)_2\text{Pt}(\text{L}_2)]^{n-}$ ($\text{L}_2 = \text{acac}$, $n = 1$; $\text{L} = \text{CH}_3\text{CN}$, $n = 0$) complexes and their behavior toward Ag(I) and I_2 .

Results and Discussion

Synthesis of $[\text{NBu}_4][(\text{R}_F)_2\text{Pt}(\mu\text{-PPh}_2)_2\text{Pt}(\mu\text{-PPh}_2)_2\text{Pt}(\text{acac})]$. The Oxidation with Ag(I). Some of the complexes used in this study as starting materials had not been prepared before, and their syntheses is described first (**4**, **5**, and **10**). Their structural characterization was carried out by usual methods (infrared (IR), nuclear magnetic resonance (NMR), and X-ray diffraction (XRD), in some cases). A schematic representation of their structures is given in Scheme 1, and for the sake of clarity, the structural parameters are commented on all together.

The reaction of acetone solutions of the trinuclear complex $[\text{NBu}_4]_2[(\text{R}_F)_2\text{Pt}(\mu\text{-PPh}_2)_2\text{Pt}(\mu\text{-PPh}_2)_2\text{Pt}(\text{R}_F)_2]^{3-}$ (**1**) with $\text{HCl}_{(\text{aq})}$ (1:2 molar ratio) was the procedure used for the preparation of the hexanuclear derivative $[\text{NBu}_4]_2\{[(\text{R}_F)_2\text{Pt}(\mu\text{-PPh}_2)_2\text{Pt}(\mu\text{-PPh}_2)_2\text{Pt}(\mu\text{-Cl})]\}_2$ (**4**). In this process, two Pt– C_6F_5 bonds at the same metal center are broken with the formation of two $\text{C}_6\text{F}_5\text{H}$ molecules. The intermediate $[(\text{R}_F)_2\text{Pt}(\mu\text{-PPh}_2)_2\text{Pt}(\mu\text{-PPh}_2)_2\text{PtCl}_2]^{2-}$ does not crystallize from the solution, but the elimination of a Cl^- group and dimerization of the unsaturated trinuclear fragment yields the hexanuclear $\{[(\text{R}_F)_2\text{Pt}(\mu\text{-PPh}_2)_2\text{Pt}(\mu\text{-PPh}_2)_2\text{PtCl}]\}_2^{2-}$ (**4**) instead. The XRD structure of this peculiar hexanuclear anionic complex is discussed below. The “Pt($\mu\text{-Cl}$) $_2$ Pt” bridging system is expected to be

(3) Alonso, E.; Casas, J. M.; Forniés, J.; Fortuño, C.; Martín, A.; Orpen, A. G.; Tsiapis, C. A.; Tsiapis, A. C. *Organometallics* **2001**, *20*, 5571–5582.

(4) Forniés, J.; Fortuño, C.; Ibáñez, S.; Martín, A. *Inorg. Chem.* **2006**, *45*, 4850–4858.

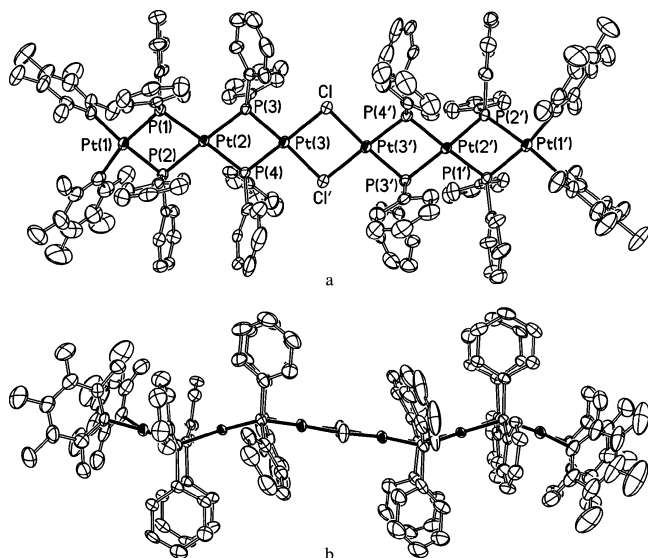


Figure 1. Molecular structure of the anion of complex $[\text{NBu}_4][\{(\text{R}_F)_2\text{Pt}(\mu\text{-PPh}_2)_2\text{Pt}(\mu\text{-Cl})\}_2] \cdot 5.5\text{Me}_2\text{CO}$ (**4** · 5.5Me₂CO).

easily split, and thus this hexanuclear complex, **4**, represents an excellent starting material for the synthesis of unsymmetrical trinuclear phosphido-bridged derivatives. Complex **4** reacts with $\text{Ti}(\text{acac})$ (1:2 molar ratio), and after the elimination of TiCl , the trinuclear complex $[\text{NBu}_4][(\text{R}_F)_2\text{Pt}(\mu\text{-PPh}_2)_2\text{Pt}(\mu\text{-PPh}_2)_2\text{Pt}(\text{acac})]$ (**5**) is crystallized (Scheme 1). This reaction is reversible, and the addition of HCl solutions to **5** (1:1 molar ratio) yields back the hexanuclear complex **4**.

The addition of AgClO_4 to **5** (2:1 molar ratio) results in the precipitation of Ag^0 and the formation of the cationic complex $[(\text{R}_F)_2\text{Pt}(\mu\text{-PPh}_2)_2\text{Pt}(\mu\text{-PPh}_2)_2\text{Pt}(\text{acac})][\text{ClO}_4]$ (**6**; Pt(I-II), Pt(III), Pt(II), Scheme 1), which is isolated from the solution. The reaction of **5** (48 valence electron count) with Ag^+ results in an oxidation process which affords the trinuclear complex **6**, of 46 valence electrons, with formally two platinum(III) metal centers joined by a metal–metal bond located in the fragment “ $(\text{R}_F)_2\text{Pt}(\mu\text{-PPh}_2)_2\text{Pt}$ ”. It is noteworthy that the binuclear acac derivative $[(\text{R}_F)_2\text{Pt}(\mu\text{-PPh}_2)_2\text{Pt}(\text{acac})]^-$ reacts with Ag^+ , yielding stable platinum(II)–silver(I) bonds, while from the similar trinuclear acac derivative **5**, the platinum(II)–silver(I) adduct evolves with electron transfer, yielding **6**.² This oxidation process is reversible, and the addition of NBu_4BH_4 to solutions of **6** gives back the platinum(II) complex **5**.

Structural Characterization of Complexes 4, 5, and 6. X-Ray Studies. The crystal structures of complexes **4**, **5**, and **6** have been determined by single-crystal X-ray diffraction. The structures of the anions are shown in Figures 1, 2, and 3, respectively. Tables 1, 2, and 3 collect some relevant bond distances and angles. In the case of **4**, the structural determination confirms its hexanuclear nature, with the six Pt atoms disposed in an almost linear array. The anion has an inversion center, and thus both halves of the molecule are equivalent. The terminal Pt(1) has two pentafluorophenyl terminal ligands and two PPh_2 groups, which are acting as a bridge with Pt(2). Also, this Pt(2) center is joined to Pt(3) through two diphenylphosphido bridging ligands. Pt(3) is

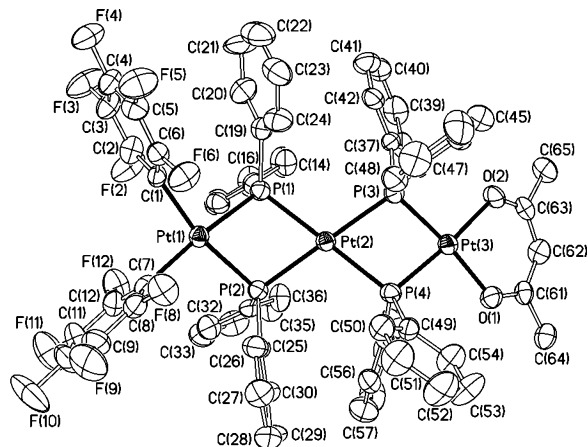


Figure 2. Molecular structure of the anion of complex $[\text{NBu}_4][(\text{R}_F)_2\text{Pt}(\mu\text{-PPh}_2)_2\text{Pt}(\mu\text{-PPh}_2)_2\text{Pt}(\text{acac})] \cdot 2\text{Me}_2\text{CO}$ (**5** · 2Me₂CO).

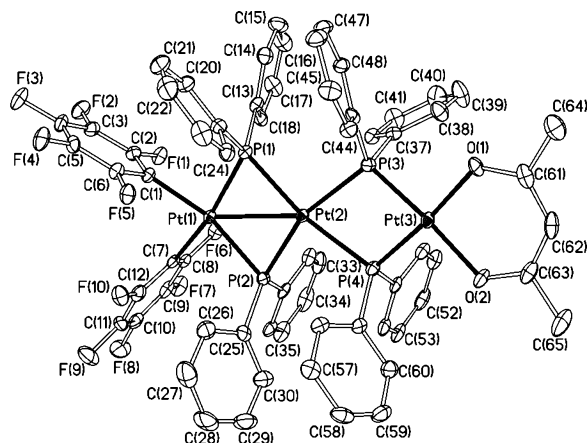


Figure 3. Molecular structure of the complex in $[(\text{R}_F)_2\text{Pt}(\mu\text{-PPh}_2)_2\text{Pt}(\mu\text{-PPh}_2)_2\text{Pt}(\text{acac})][\text{ClO}_4] \cdot 3\text{CH}_2\text{Cl}_2$ (**6** · 3CH₂Cl₂).

Table 1. Selected Bond Distances (Å) and Angles (deg) for $[\text{NBu}_4][\{(\text{R}_F)_2\text{Pt}(\mu\text{-PPh}_2)_2\text{Pt}(\mu\text{-PPh}_2)_2\text{Pt}(\mu\text{-Cl})\}_2] \cdot 5.5\text{Me}_2\text{CO}$ (**4** · 5.5Me₂CO)^a

Pt(1)–C(7)	2.070(10)	Pt(1)–C(1)	2.072(8)
Pt(1)–P(2)	2.292(2)	Pt(1)–P(1)	2.311(2)
Pt(2)–P(4)	2.318(2)	Pt(2)–P(2)	2.331(2)
Pt(2)–P(3)	2.336(2)	Pt(2)–P(1)	2.356(2)
Pt(3)–P(4)	2.237(2)	Pt(3)–P(3)	2.248(2)
Pt(3)–Cl'	2.418(2)	Pt(3)–Cl	2.421(2)
C(7)–Pt(1)–C(1)	90.1(3)	C(7)–Pt(1)–P(2)	95.0(2)
C(1)–Pt(1)–P(2)	174.9(2)	C(7)–Pt(1)–P(1)	169.0(3)
C(1)–Pt(1)–P(1)	99.7(2)	P(2)–Pt(1)–P(1)	75.19(7)
P(4)–Pt(2)–P(2)	103.73(8)	P(4)–Pt(2)–P(3)	74.36(7)
P(2)–Pt(2)–P(3)	176.20(7)	P(4)–Pt(2)–P(1)	177.02(8)
P(2)–Pt(2)–P(1)	73.64(7)	P(3)–Pt(2)–P(1)	108.17(7)
P(4)–Pt(3)–P(3)	77.68(8)	P(4)–Pt(3)–Cl'	97.98(8)
P(3)–Pt(3)–Cl'	175.45(8)	P(4)–Pt(3)–Cl	178.01(8)
P(3)–Pt(3)–Cl	100.83(8)	Cl'–Pt(3)–Cl	83.49(8)
Pt(3')–Cl–Pt(3)	96.51(8)	Pt(1)–P(1)–Pt(2)	97.15(8)
Pt(1)–P(2)–Pt(2)	98.41(8)	Pt(3)–P(3)–Pt(2)	99.91(8)
Pt(3)–P(4)–Pt(2)	100.80(8)		

^a Symmetry transformation used to generate equivalent primed atoms: $-x, -y, -z$.

joined with its symmetry equivalent, Pt(3'), by two bridging chloro ligands. The Pt···Pt distances are large (range from 3.500(1) Å to 3.610(1) Å) and clearly indicate the absence of any metal–metal interaction, as expected for a saturated species with a 96 valence electron count (VEC). The environments of the Pt atoms are square-planar, with the P–Pt–P and Pt–P–Pt angles typically found in these kinds

Table 2. Selected Bond Distances (Å) and Angles (deg) for [NBu₄][(R_F)₂Pt(μ-PPh₂)₂Pt(μ-PPh₂)₂Pt(acac)]·2Me₂CO (5·2Me₂CO)

Pt(1)–C(7)	2.057(8)	Pt(1)–C(1)	2.062(7)
Pt(1)–P(1)	2.2796(18)	Pt(1)–P(2)	2.3086(19)
Pt(2)–P(4)	2.328(2)	Pt(2)–P(3)	2.333(2)
Pt(2)–P(1)	2.3428(19)	Pt(2)–P(2)	2.3529(19)
Pt(3)–O(1)	2.068(5)	Pt(3)–O(2)	2.102(5)
Pt(3)–P(4)	2.2258(19)	Pt(3)–P(3)	2.237(2)
C(7)–Pt(1)–C(1)	92.5(3)	C(7)–Pt(1)–P(1)	173.4(2)
C(1)–Pt(1)–P(1)	93.54(19)	C(7)–Pt(1)–P(2)	99.0(2)
C(1)–Pt(1)–P(2)	167.86(19)	P(1)–Pt(1)–P(2)	75.16(7)
P(4)–Pt(2)–P(3)	73.62(7)	P(4)–Pt(2)–P(1)	173.11(7)
P(3)–Pt(2)–P(1)	107.43(7)	P(4)–Pt(2)–P(2)	105.74(7)
P(3)–Pt(2)–P(2)	179.26(8)	P(1)–Pt(2)–P(2)	73.15(7)
O(1)–Pt(3)–O(2)	88.36(19)	O(1)–Pt(3)–P(4)	94.90(14)
O(2)–Pt(3)–P(4)	173.09(15)	O(1)–Pt(3)–P(3)	172.18(14)
O(2)–Pt(3)–P(3)	99.41(15)	P(4)–Pt(3)–P(3)	77.48(7)
Pt(1)–P(1)–Pt(2)	101.16(7)	Pt(1)–P(2)–Pt(2)	100.00(7)
Pt(3)–P(3)–Pt(2)	101.88(8)	Pt(3)–P(4)–Pt(2)	102.40(7)

Table 3. Selected Bond Distances (Å) and Angles (deg) for [(R_F)₂Pt(μ-PPh₂)₂Pt(μ-PPh₂)₂Pt(acac)][ClO₄]·3CH₂Cl₂ (6·3CH₂Cl₂)

Pt(1)–C(1)	2.064(4)	Pt(1)–C(7)	2.090(4)
Pt(1)–P(1)	2.2655(13)	Pt(1)–P(2)	2.2664(12)
Pt(1)–Pt(2)	2.7633(3)	Pt(2)–P(2)	2.3108(13)
Pt(2)–P(1)	2.3247(13)	Pt(2)–P(3)	2.3678(12)
Pt(2)–P(4)	2.3934(12)	Pt(3)–O(2)	2.064(3)
Pt(3)–O(1)	2.066(3)	Pt(3)–P(3)	2.2129(13)
Pt(3)–P(4)	2.2226(13)		
C(1)–Pt(1)–C(7)	84.79(17)	C(1)–Pt(1)–P(1)	85.83(13)
C(7)–Pt(1)–P(1)	166.33(13)	C(1)–Pt(1)–P(2)	165.05(13)
C(7)–Pt(1)–P(2)	83.07(12)	P(1)–Pt(1)–P(2)	107.57(4)
P(2)–Pt(2)–P(1)	104.14(4)	P(2)–Pt(2)–P(3)	160.64(4)
P(1)–Pt(2)–P(3)	94.15(4)	P(2)–Pt(2)–P(4)	89.89(4)
P(1)–Pt(2)–P(4)	165.65(4)	P(3)–Pt(2)–P(4)	72.29(4)
O(2)–Pt(3)–O(1)	90.01(13)	O(2)–Pt(3)–P(3)	173.48(10)
O(1)–Pt(3)–P(3)	96.02(10)	O(2)–Pt(3)–P(4)	95.45(10)
O(1)–Pt(3)–P(4)	174.45(10)	P(3)–Pt(3)–P(4)	78.56(5)
Pt(1)–P(1)–Pt(2)	74.01(4)	Pt(1)–P(2)–Pt(2)	74.27(4)
Pt(3)–P(3)–Pt(2)	104.02(5)	Pt(3)–P(4)–Pt(2)	102.89(5)

of bridging systems with no metal–metal bonds. The Pt square planes are not coplanar but establish a sort of zigzag setup (see Figure 1b). Thus, the Pt(1) plane and the Pt(2) plane form a dihedral angle of 36.5(1)°, while the Pt(2) and Pt(3) planes establish a dihedral angle of 26.9(5)°. The Pt(3) and Pt(3') planes are coplanar in accordance with the molecular symmetry constraints. The topology of the cation of **4** is very remarkable, the total length of the anion being around 25.6 Å.

The structure of **5** (Figure 2) confirms that it is a trinuclear unsymmetrical complex resulting from the cleavage of the chloro bridging system in **4** and the replacement of these ligands by acac. The “(R_F)₂Pt(μ-PPh₂)₂Pt(μ-PPh₂)₂Pt” fragment is very similar to the analogous one in the precursor **4**, with the Pt atoms in square-planar environments and no Pt···Pt interactions (Pt(1)···Pt(2) = 3.571(1) Å and Pt(2)···Pt(3) = 3.549(1) Å). The environments of the Pt centers are not coplanar, the dihedral angles between the Pt(1) plane and the Pt(2) plane being 28.8(1)°, and 24.2(1)° between the Pt(2) plane and the Pt(3) plane. The acac ligand is planar and almost coplanar with the Pt(3) coordination plane (dihedral angle 13.1(1)°).

The crystal structure of complex **6** (Figure 3) shows a very short Pt(1)–Pt(2) distance, 2.763(1) Å, indicative of the existence of a metal–metal bond, as expected for a 46 VEC complex. This short distance can be compared with the separation of the analogous atoms in its precursor **5** (3.571(1)

Å) or the Pt(2)···Pt(3) distance in **6**, 3.612(1) Å, where no Pt–Pt bonds are present. The existence of the Pt(1)–Pt(2) bond in **6** also becomes apparent in the values of the P–Pt–P and Pt–P–Pt angles. Thus, the former ones take broad values (P(1)–Pt(1)–P(2) = 107.6(1)°, P(1)–Pt(2)–P(2) = 104.1(1)°; cf. 75.2(1)° and 73.2(1)°, respectively, in **5**), while the latter ones are more acute (Pt(1)–P(1)–Pt(2) = 74.0(4)°, Pt(1)–P(2)–Pt(2) = 74.3(4)°; cf. 101.2(1)° and 100.0(1)°, respectively, in **5**). The analogous angles in **6** involving Pt(2), Pt(3), P(3), and P(4) are typical for a “Pt(μ-PPh₂)₂Pt” bridging system with no Pt–Pt bond and are very similar to the analogous values found in the precursor **5**.

Another structural difference between complexes **5** and **6** is their overall shape, since while in **5** the environment of the Pt centers is not coplanar, the existence of the Pt(1)–Pt(2) bond in **6** causes its core to be nearly planar. Thus, the dihedral angle between the Pt(1) and Pt(2) square planes is only 3.5(1)°, while the dihedral angle between the Pt(2) and Pt(3) planes is 14.0(1)° (compare with 28.8(1)° and 24.2(1)° for **5**). A common feature for **5** and **6** is that the acac ligand is planar, and almost coplanar with the Pt(3) plane, the corresponding dihedral angle being 13.1(1)° in **5** and 5.1(1)° in **6**.

Spectroscopic Studies. The IR spectra of **4–6** show two absorptions in the 800 cm⁻¹ region, in agreement with the maintenance of the *cis*-“Pt(C₆F₅)₂” fragment,^{5,6} and for **5** and **6** two absorptions in the 1600–1500 cm⁻¹ due to the presence of the acac ligand. The absorption in the 950 cm⁻¹ region due to the C₆F₅ groups appears at 965 cm⁻¹ in **6**, while in the precursor **5**, it appears at 949 cm⁻¹. The displacement toward higher frequencies of this absorption has been largely related with the increase in the oxidation state of the metal bonded to the C₆F₅ groups,^{1,3,6,7} and this is also in agreement with the formal oxidation states of the Pt centers bonded to C₆F₅ in **5** and **6**.

The ¹H NMR spectra of **4–6** in solution show signals due to the phenyl H atoms and for **4** and **5** those expected for the NBu₄⁺ counterion. Complexes **5** and **6** show two singlets at *ca.* 5.0 and 1.5 ppm (1:6 intensity ratio) due to the acac ligand.

The ¹⁹F NMR spectra of **4** and **5** show three signals due to the *o*-F, *m*-F, and *p*-F. This pattern is in agreement with the equivalence of the C₆F₅ groups in the complexes and the equivalence of the two *o*-F atoms, as well as the two *m*-F atoms, within each ring. The P atoms in **4** and **5** appear as an AA'XX' spin system in the ³¹P{¹H} NMR spectra of the isotopologues not having ¹⁹⁵Pt. The high-field chemical shifts at δ -113.0 and -132.5 are in agreement with the presence of “Pt(μ-PPh₂)₂Pt” fragments with non bonding platinum–platinum distances.^{3,8–12} The AA' part (δ -113.0)

(5) Maslowsky, E. J. *Vibrational Spectra of Organometallic Compounds*; Wiley: New York, 1997.

(6) Usón, R.; Forniés, J. *Adv. Organomet. Chem.* **1988**, *28*, 219–297.

(7) Alonso, E.; Forniés, J.; Fortuño, C.; Martín, A.; Orpen, A. G. *Organometallics* **2001**, *20*, 850–859.

(8) Carty, A. J.; MacLaughlin, S. A.; Nucciarone, D. *Phosphorus-31 NMR Spectroscopy in Stereochemical Analysis*; VCH: New York, 1987.

(9) Ara, I.; Chaouche, N.; Forniés, J.; Fortuño, C.; Kribii, A.; Martín, A. *Eur. J. Inorg. Chem.* **2005**, *389*, 4–3901.

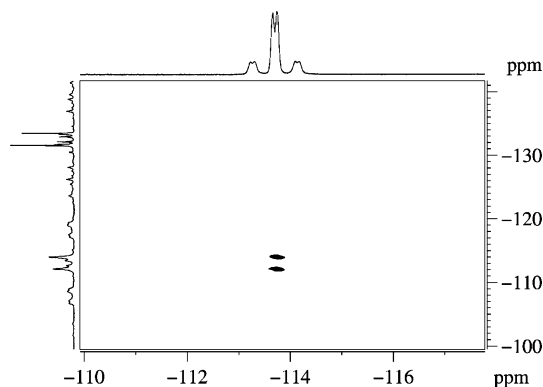


Figure 4. ^{19}F – ^{31}P HMQC spectrum of **5** (acetone- d_6 , 295 K).

is broader than its XX' counterpart (δ –132.5), suggesting that A and A' are to be assigned to the P atoms trans to the C_6F_5 groups. This was validated by the ^{19}F – ^{31}P heteronuclear multiple-quantum coherence (HMQC) spectrum showing the correlation between the *o*-F and the ^{31}P nuclei at δ –113.0 (Figure 4 and Figure S3, Supporting Information).

All ^{31}P features of **4** and **5** (see Experimental Section) were determined by computer simulation of the AA'XX' (29.0%), AA'XX'M (14.8% for each of the three isotopomers), and AA'XX'MM' (7.6% for each of the three isotopomers) spin systems (A and X = ^{31}P ; M = ^{195}Pt), using as starting chemical shifts and coupling constants those extractable directly from the experimental $^{31}\text{P}\{^1\text{H}\}$ and $^{31}\text{P}\{^1\text{H}\}$ correlation spectroscopy (COSY) NMR spectra (Figure 5, Figures S1 and S5, Supporting Information). In particular, the tilts of the cross-peaks in the $^{31}\text{P}\{^1\text{H}\}$ COSY spectra allowed us to unequivocally determine the 1J or $^2J_{\text{P,Pt}}$ values that were not directly extractable from 1D spectra due to overlapping of the ^{195}Pt satellites.

The $^{195}\text{Pt}\{^1\text{H}\}$ NMR spectra of **4** and **5** (Figures S2 and S6, Supporting Information) show three signals: a triplet (δ –3357 for **4** and δ –3159 for **5**) assigned to the Pt^3 atoms (bound to Cl and acac, respectively), a triplet of triplets (δ –3857 for **4** and δ –894 for **5**) arising from the “ $(\mu\text{-PPh}_2)_2\text{Pt}^2(\mu\text{-PPh}_2)_2$ ” fragment, and a multiplet (δ –3795 for **4** and δ –3793 for **5**) assigned to the Pt^1 (bearing the C_6F_5 groups). The broadness of the latter signals is mainly due to the scalar coupling between ^{195}Pt and ^{19}F atoms. The ^{19}F – ^{195}Pt HMQC spectrum of **5** (Figure 6) shows that Pt^1 is scalarly coupled with the *o*-F ($^3J_{\text{F,Pt}} = 330$ Hz) as well as with the *m*-F (ca. 2 Hz).

The increase in the formal oxidation state of Pt^1 and Pt^2 atoms passing from **5** [$\text{Pt}^1(\text{II})$ – $\text{Pt}^2(\text{II})$ – $\text{Pt}^3(\text{II})$] to **6** [$\text{Pt}^1(\text{III})$ – $\text{Pt}^2(\text{III})$ – $\text{Pt}^3(\text{II})$] is accompanied by significant changes of the ^{31}P and ^{195}Pt NMR features. The $^{31}\text{P}\{^1\text{H}\}$ NMR spectrum of **6** contains signals centered at δ 268.6 and δ –137.2 (Figures S7 and S8, Supporting Information). The chemical shift of P atoms of the “ $\text{Pt}^1(\mu\text{-PPh}_2)_2\text{Pt}^2$ ” fragment is strongly low-field-shifted in **6** (δ 268.6) with

respect to the anionic starting material **5** (δ –113.0), in agreement with the shorter intermetallic distances between $\text{Pt}^1(\text{III})$ and $\text{Pt}^2(\text{III})$.^{8,13} The $^{195}\text{Pt}\{^1\text{H}\}$ NMR signals (Figure S9, Supporting Information) of the Pt^3 atoms (i.e., the ones remaining in the formal oxidation state +2) are almost unchanged (δ –3159 in **5** and δ –3087 in **6**), whereas those of the other $\text{Pt}^{\text{I or 2}}$ atoms become more shielded passing from **5** to **6**. In particular, the triplet of triplets attributable to Pt^2 is shifted by ca. 900 ppm to higher fields passing from δ –3894 in **5** to δ –4809 in **6**, while the Pt^1 multiplet results are high-field-shifted by almost 1500 ppm (δ –3793 in **5** and δ –5279 in **6**). The strong shielding found for ^{195}Pt nuclei upon increasing the oxidation state deserves a comment. In fact, it has been reported^{14–16} that the oxidation from Pt(II) to Pt(III) causes a deshielding of the ^{195}Pt nuclei (Table 4) ranging from 903 to 2182 ppm.

However, in the literature examples shown in Table 4, the change of oxidation state occurs with a change of complex geometry (from square-planar to octahedral), which is known to affect the ^{195}Pt chemical shift.¹⁷ Thus, in order to confirm the effect on δ_{Pt} of the +2 \rightarrow +3 oxidation for square-planar complexes not undergoing a geometry change upon removal of the electrons, we recorded the $^{195}\text{Pt}\{^1\text{H}\}$ NMR spectra of complexes $[(\text{R}_\text{F})_2\text{Pt}^{\text{III}}(\mu\text{-PPh}_2)_2\text{Pt}^{\text{III}}(\text{R}_\text{F})_2]$ and **2** (Scheme 1) and compared the obtained δ_{Pt} values with those of their Pt(II) precursors $[(\text{R}_\text{F})_2\text{Pt}^{\text{II}}(\mu\text{-PPh}_2)_2\text{Pt}^{\text{II}}(\text{R}_\text{F})_2]^{2-}$ and **1**, respectively. The values shown in Table 4 indicate that for square-planar Pt(III) complexes the increase of oxidation state results, in all cases, in a strong shielding of the ^{195}Pt nuclei. Although it is premature to draw conclusions on the basis of only those few examples, it seems that the geometry around the Pt atoms (in particular, the presence of the Pt_2P_2 ring endowed with a Pt–Pt bond) plays a role in its chemical shift. Further studies are warranted to gain insights on this topic.

The few platinum(III) or palladium(III) binuclear phosphido derivatives that we have prepared behave as intermediates for platinum(II) or palladium(II) complexes through reductive coupling processes with the formation of P–C or P–P bonds.^{4,18–20} Aiming to study the stability of the platinum(III) complex **6**, we recorded the ^{19}F and $^{31}\text{P}\{^1\text{H}\}$ NMR spectra of a deuteriochloroform solution of **6** after 24, 48, and 72 h at room temperature. These spectra showed a great number of signals, indicating the disappearance of **6** and the presence of mixtures of complexes that we have not been able to identify, although signals due to the presence

(10) Alonso, E.; Forniés, J.; Fortuño, C.; Tomás, M. *J. Chem. Soc., Dalton Trans.* **1995**, 3777–3784.
 (11) Forniés, J.; Fortuño, C.; Gil, R.; Martín, A. *Inorg. Chem.* **2005**, *44*, 9534–9541.
 (12) Falvello, L. R.; Forniés, J.; Fortuño, C.; Durán, F.; Martín, A. *Organometallics* **2002**, *21*, 2226–2234.

(13) Falvello, L. R.; Forniés, J.; Fortuño, C.; Martínez, F. *Inorg. Chem.* **1994**, *33*, 6242–6246.
 (14) King, C.; Roundhill, D. M.; Dickson, M. K.; Fronczek, F. R. *J. Chem. Soc., Dalton Trans.* **1987**, 2769–2780.
 (15) O'Halloran, T. V.; Roberts, M. M.; Lippard, S. J. *Inorg. Chem.* **1986**, *25*, 957–964.
 (16) Whitfield, S. R.; Sanford, M. S. *Organometallics* **2008**, *27*, 1683–1689.
 (17) Pregosin, P. S. *Coord. Chem. Rev.* **1982**, *44*, 247–291.
 (18) Chaouche, N.; Forniés, J.; Fortuño, C.; Kribii, A.; Martín, A.; Karipidis, P.; Tsepis, A. C.; Tsepis, C. A. *Organometallics* **2004**, *23*, 1797–1810.
 (19) Ara, I.; Chaouche, N.; Forniés, J.; Fortuño, C.; Kribii, A.; Tsepis, A. C. *Organometallics* **2006**, *25*, 1084–1091.
 (20) Forniés, J.; Fortuño, C.; Ibáñez, S.; Martín, A.; Tsepis, A. C.; Tsepis, C. A. *Angew. Chem., Int. Ed.* **2005**, *44*, 2407–2410.

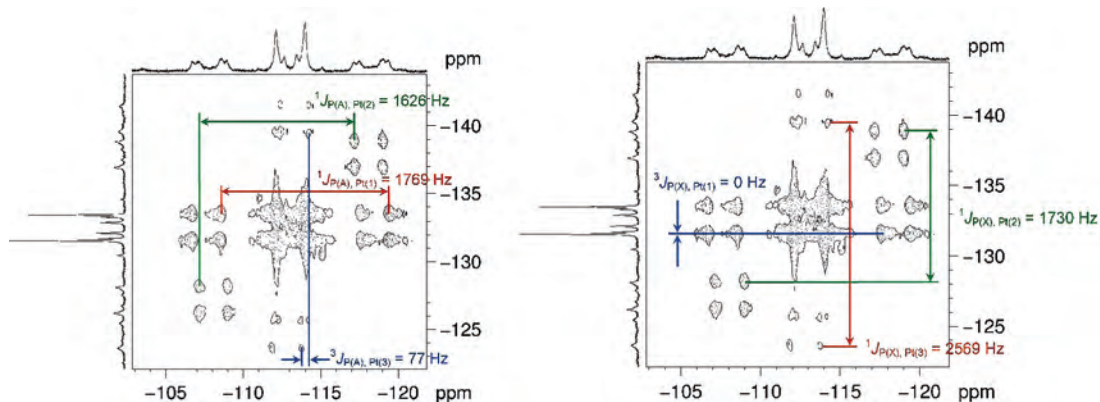


Figure 5. $^{31}\text{P}\{^1\text{H}\}$ COSY spectra of **5** (acetone- d_6 , 295 K).

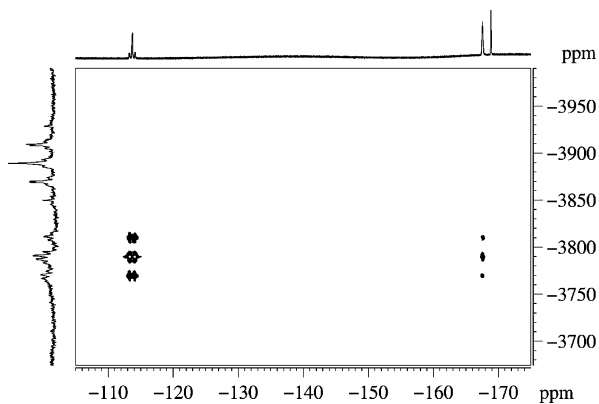


Figure 6. ^{19}F – ^{195}Pt HMQC spectrum of **5** (acetone- d_6 , 295 K).

of the PPh_2R_F ligand were identified. It is worth noting that complex **6** is related to complex **2** since both derivatives show a linear arrangement of the three metal centers, a 46 valence electron count, and a Pt(III)–Pt(III) bond in the analogous “ $(\text{R}_F)_2\text{Pt}(\mu\text{-PPh}_2)_2\text{Pt}$ ” fragment. Complex **2** is stable at room temperature, but upon heating, it evolves toward the Pt(II) derivative **3**, with the formation of a P–C bond. Complex **2** reacts with bromide to produce a binuclear Pt(II) bromo derivative with PPh_2R_F through a reductive P–C coupling.⁴ Because of that, we have studied the behavior of trinuclear complex **6** toward bromide.

Reaction of Complex 6 with NBu_4Br . The reaction of the orange complex **6** with Br^- (1:1 molar ratio) at room temperature yields a yellow solid identified as a mixture of isomers of stoichiometry $[(\text{PPh}_2\text{R}_F)(\text{R}_F)\text{Pt}(\mu\text{-PPh}_2)(\mu\text{-Br})\text{Pt}(\mu\text{-PPh}_2)_2\text{Pt}(\text{acac})]$ (**7a,b**, Scheme 1), which are the result of the coupling between a C_6F_5 group bonded to a Pt(III) center and a bridging PPh_2 ligand. Although we have not been able to separate the isomers, two fractions of the yellow solid with different **7a/7b** ratios were obtained, and we have identified each isomer by spectroscopic means (see the Experimental Section). Both the ^{19}F NMR spectra of **7a** and **7b** show six signals in a 2:2.1:2:1:2 intensity ratio (see the Experimental Section), in agreement with the presence of two kinds of pentafluorophenyl groups and the equivalence of the two *o*-F atoms, as well as the *m*-F atoms, within each ring. The different chemical shifts of the F atoms of C_6F_5 groups bonded to the platinum center or to the phosphorus atom allow the unequivocal assignment of these signals (see

the Experimental Section).^{18,19,21} The $^{31}\text{P}\{^1\text{H}\}$ NMR spectra of **7a** and **7b** are conclusive in ascertaining their structures, and all data extracted from the spectra are given in the Experimental Section (see Scheme 1 for atom numbering). The signals due to the P4 (doublet of doublets) and the P3 (doublet) atoms appear at high field (from -132.9 to -146.5 ppm), in the range expected for two PPh_2 groups bonding to two metal centers not joined by a metal–metal bond.^{3,4,8–11,22} The signal due to P1 appears as a doublet of doublets (**7a**) or as a doublet (**7b**) at -31.3 or -37.9 , respectively, in the range expected for this “ $\text{Pt}(\mu\text{-PPh}_2)(\mu\text{-Br})\text{Pt}$ ” fragment in a saturated complex.^{10,11,18,19,23,24} Finally, the signal due to P2 appears as a doublet or as a singlet.

Oxidation Processes with I_2 . In order to determine the influence of the oxidizing agent on the oxidation of **5**, we have studied the addition of I_2 to CH_2Cl_2 solutions of **5** (1:1 molar ratio). After workup, the hexanuclear Pt(II) complex $[(\text{PPh}_2\text{R}_F)(\text{R}_F)\text{Pt}(\mu\text{-PPh}_2)(\mu\text{-I})\text{Pt}(\mu\text{-PPh}_2)_2\text{Pt}(\mu\text{-I})_2]$ (**8**) is obtained (Scheme 1). The IR spectrum of **8** shows the characteristic absorptions due to the PPh_2R_F ligand (1519 , 982 cm^{-1})^{19,21} and only one signal in the 800 cm^{-1} region (*X*-sensitive, C_6F_5),^{5,6} while the absorptions due to the acac ligand are absent. The ^{19}F NMR and $^{31}\text{P}\{^1\text{H}\}$ NMR spectra of **8** in deuteroacetone show the same pattern as for complex **7a**, and all data extracted from the spectra are given in the Experimental Section. Unfortunately, we have not been able to obtain suitable crystals of **8** for X-ray studies in order to establish unequivocally the hexanuclear nature of **8**, but the reaction of **8** with PPh_3 (1:2 molar ratio) yields $[(\text{PPh}_2\text{R}_F)(\text{R}_F)\text{Pt}(\mu\text{-PPh}_2)(\mu\text{-I})\text{Pt}(\mu\text{-PPh}_2)_2\text{PtI}(\text{PPh}_3)]$, **9**, through the expected cleavage process of the $\text{Pt}(\mu\text{-I})_2\text{Pt}$ bridging system. Complex **9** has been fully characterized by IR,¹⁹ ^{19}F NMR, $^{31}\text{P}\{^1\text{H}\}$ NMR, and $^{195}\text{Pt}\{^1\text{H}\}$ NMR spectroscopy (see the Experimental Section) and single-crystal X-ray diffraction. The structure of **9** is shown in Figure 7. Selected bond distances and angles are listed in Table 5. As can be seen, **9** is a trinuclear complex in which the three Pt atoms are held

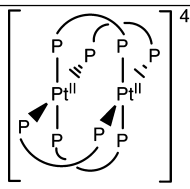
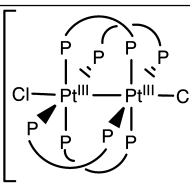
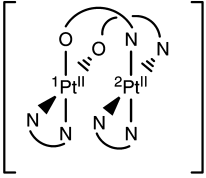
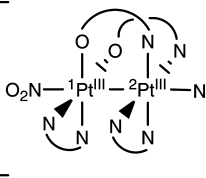
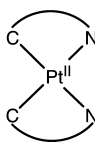
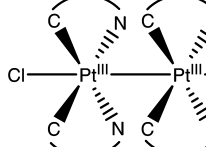
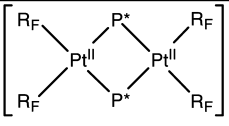
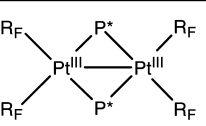
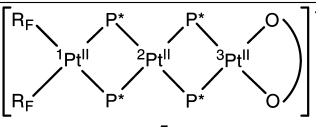
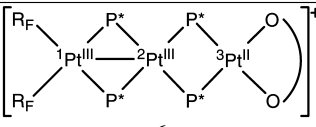
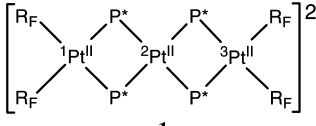
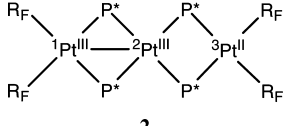
(21) Falvello, L. R.; Forniés, J.; Fortuño, C.; Martín, A.; Martínez-Sariñena, A. P. *Organometallics* **1997**, *16*, 5849–5856.

(22) Forniés, J.; Fortuño, C.; Navarro, R.; Martínez, F.; Welch, A. J. J. *Organomet. Chem.* **1990**, *394*, 643–658.

(23) Ara, I.; Chaouche, N.; Forniés, J.; Fortuño, C.; Kribii, A.; Tsipis, A. C.; Tsipis, C. A. *Inorg. Chim. Acta* **2005**, *358*, 1377–1385.

(24) Alonso, E.; Forniés, J.; Fortuño, C.; Martín, A.; Rosair, G. M.; Welch, A. J. *Inorg. Chem.* **1997**, *36*, 4426–4431.

Table 4. Values of Chemical Shifts (ppm) of ^{195}Pt in Pt(II), Octahedral Pt(III), and Square-Planar Pt(III) Complexes

δ_{Pt}	δ_{Pt}	$\delta_{\text{Pt(III)}} - \delta_{\text{Pt(II)}}$	Ref.
 -5139	 -4236	903	14
 $\text{Pt}^1 = -1639$ $\text{Pt}^2 = -2523$	 $\text{Pt}^1 = 541$ $\text{Pt}^2 = -1141\text{ppm}$	2182 1382	15
 -3542	 -2293	1249	16
 -3795	 -5298	-1503	
 5 $\text{Pt}^1 = -3793$ $\text{Pt}^2 = -3894$ $\text{Pt}^3 = -3159$	 6 $\text{Pt}^1 = -5279$ $\text{Pt}^2 = -4809$ $\text{Pt}^3 = -3087$	-1486 -915	
 1 $\text{Pt}^1 = -3751$ $\text{Pt}^2 = -3732$ $\text{Pt}^3 = -3751$	 2 $\text{Pt}^1 = -5336$ $\text{Pt}^2 = -4393$ $\text{Pt}^3 = -3783$	-1585 -661	

together through PPh_2 and I bridges. The Pt centers do not establish any kind of metal–metal interaction (48 valence electron count) as is evidenced by the $\text{Pt}\cdots\text{Pt}$ separations ($\text{Pt}(1)\cdots\text{Pt}(2)$ 3.566(1) Å, $\text{Pt}(1)\cdots\text{Pt}(2)$ 3.576(1) Å). The platinum atoms lie in the centers of square-planar environments that are not coplanar. The environment of Pt(1) is formed by a terminal pentafluorophenyl ligand, a $\text{PPh}_2(\text{C}_6\text{F}_5)$ ligand originated by a P–C coupling process of PPh_2 and C_6F_5 ligands in the precursor **8**, a PPh_2 bridging ligand, and an iodo bridging ligand trans to the C_6F_5 group. The central Pt(2) has a more distorted environment, with obtuse

P(2)–Pt(2)–P(3) and I(1)–Pt(2)–P(4) “external” angles ($106.3(1)^\circ$ and $98.2(1)^\circ$, respectively) and acute P(2)–Pt(2)–I(1) and P(3)–Pt(2)–P(4) “internal” angles ($78.8(1)^\circ$ and $76.7(1)^\circ$, respectively), as expected for a system with no Pt–Pt bonds. The square plane of Pt(1) forms a dihedral angle of $41.5(1)^\circ$ with the Pt(2) coordination plane. Again, Pt(3) shows an essentially square-planar environment, with terminal iodo and triphenylphosphine ligands, the “internal” P(3)–Pt(3)–P(4) angle being more acute, $76.4(1)^\circ$, as expected. The dihedral angle between the best square-planar environments of Pt(2) and Pt(3) is $16.6(1)^\circ$.

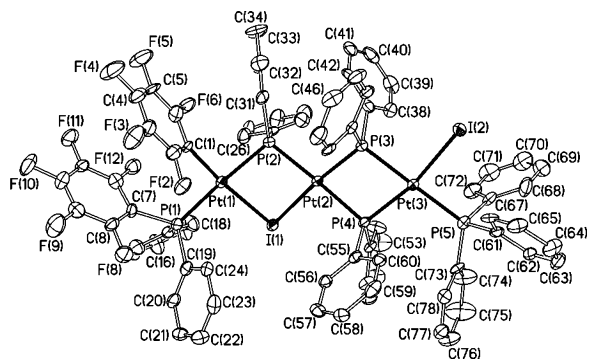


Figure 7. Molecular structure of the complex in $[(\text{PPh}_2\text{R}_f)(\text{R}_f)\text{Pt}(\mu\text{-PPh}_2)(\mu\text{-I})\text{Pt}(\mu\text{-PPh}_2)_2\text{PtI}(\text{PPh}_3)] \cdot 0.25\text{CH}_2\text{Cl}_2 \cdot 0.5n\text{-C}_6\text{H}_{14}$ (**9** · 0.25CH₂Cl₂ · 0.5n-C₆H₁₄).

Table 5. Selected Bond Distances (Å) and Angles (deg) for $[(\text{PPh}_2\text{R}_f)(\text{R}_f)\text{Pt}(\mu\text{-PPh}_2)(\mu\text{-I})\text{Pt}(\mu\text{-PPh}_2)_2\text{PtI}(\text{PPh}_3)] \cdot 0.25\text{CH}_2\text{Cl}_2 \cdot 0.5n\text{-C}_6\text{H}_{14}$ (**9** · 0.25CH₂Cl₂ · 0.5n-C₆H₁₄)

Pt(1)–C(1)	2.002(9)	Pt(1)–P(1)	2.293(3)
Pt(1)–P(2)	2.313(3)	Pt(1)–I(1)	2.6779(7)
Pt(2)–P(3)	2.259(3)	Pt(2)–P(4)	2.319(3)
Pt(2)–P(2)	2.361(3)	Pt(2)–I(1)	2.6872(7)
Pt(3)–P(4)	2.272(2)	Pt(3)–P(3)	2.320(2)
Pt(3)–P(5)	2.336(2)	Pt(3)–I(2)	2.6436(7)
C(1)–Pt(1)–P(1)	92.0(3)	C(1)–Pt(1)–P(2)	94.6(3)
P(1)–Pt(1)–P(2)	171.33(10)	C(1)–Pt(1)–I(1)	170.4(3)
P(1)–Pt(1)–I(1)	94.36(7)	P(2)–Pt(1)–I(1)	79.78(6)
P(3)–Pt(2)–P(4)	76.65(8)	P(3)–Pt(2)–P(2)	106.28(9)
P(4)–Pt(2)–P(2)	176.86(9)	P(3)–Pt(2)–I(1)	173.73(6)
P(4)–Pt(2)–I(1)	98.23(6)	P(2)–Pt(2)–I(1)	78.77(6)
P(4)–Pt(3)–P(3)	76.38(8)	P(4)–Pt(3)–P(5)	103.08(9)
P(3)–Pt(3)–P(5)	173.79(9)	P(4)–Pt(3)–I(2)	167.45(6)
P(3)–Pt(3)–I(2)	91.42(6)	P(5)–Pt(3)–I(2)	89.37(7)
Pt(1)–I(1)–Pt(2)	83.32(2)		

The formation of **8** can be envisaged as the result of the oxidation of **5** probably with the formation of the intermediate **6** and two I[−] anions. The presence of I[−] favors the reductive coupling of PPh₂ and R_f (formation of the PPh₂R_f ligand). Surprisingly, one I[−] replaces the chelating acac ligand, and the dimerization of the trinuclear unsaturated fragments through the formation of the Pt(μ-I)₂Pt system produces the hexanuclear complex **8**.²⁵

Finally, we have prepared the neutral unsymmetrical trinuclear complex $[(\text{R}_f)_2\text{Pt}(\mu\text{-PPh}_2)_2\text{Pt}(\mu\text{-PPh}_2)_2\text{Pt}(\text{NCMe})_2]$ (**10**) and studied its behavior toward I₂ in order to prepare a Pt(III) iodo derivative (considering the lability of the CH₃CN ligands) and study its evolution by raising the temperature.

The synthesis of **10** has been carried out by protonation with HClO₄ of the acac ligand in **5** in the presence of acetonitrile (Scheme 1). All data extracted from the IR and NMR spectra of **10** are in agreement with the proposed formula and are collected in the Experimental Section. The ³¹P{¹H} NMR signals in DMF (295 K) fall at −119.2 and −127.7, while the ¹⁹⁵Pt{¹H} NMR signals for Pt^I, Pt², and Pt³ fall at δ −3773, δ −3881, and δ −3461, respectively.

The reaction of complex **10** with I₂ in CH₂Cl₂/MeCN (1:1

(25) According to reviewer's suggestion, we have studied the room temperature reaction of I[−] with **6** in CH₂Cl₂. To a suspension of 75 mg of **6** in 10 mL of CH₂Cl₂ was added NBU₄I (46 mg). The solution was stirred for 30 h at room temperature and passed through a silica gel column. The yellow solution was evaporated to ca. 1 mL and ^tPrOH was added. A yellow solid crystallized, which was identified (IR and ¹⁹F NMR) as complex **8**.

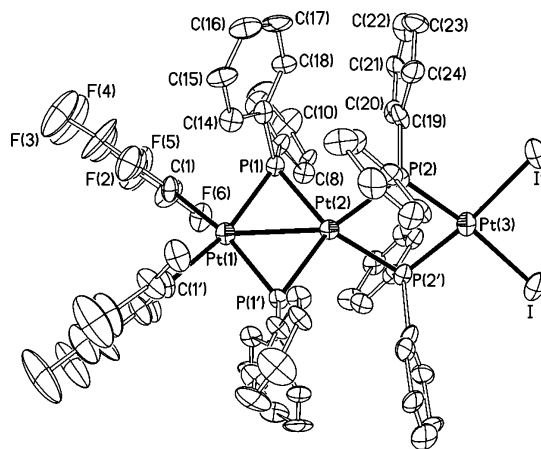


Figure 8. Molecular structure of the complex in $[(\text{R}_f)_2\text{Pt}(\mu\text{-PPh}_2)_2\text{Pt}(\mu\text{-PPh}_2)_2\text{PtI}_2] \cdot 2\text{CH}_2\text{Cl}_2 \cdot 3\text{H}_2\text{O}$ (**11** · 2CH₂Cl₂ · 3H₂O).

Table 6. Selected Bond Distances (Å) and Angles (deg) for $[(\text{R}_f)_2\text{Pt}(\mu\text{-PPh}_2)_2\text{Pt}(\mu\text{-PPh}_2)_2\text{PtI}_2] \cdot 2\text{CH}_2\text{Cl}_2 \cdot 3\text{H}_2\text{O}$ (**11** · 2CH₂Cl₂ · 3H₂O)^a

Pt(1)–C(1)	2.119(17)	Pt(1)–P(1)	2.281(5)
Pt(1)–Pt(2)	2.7778(13)	Pt(2)–P(1)	2.298(4)
Pt(2)–P(2)	2.380(4)	Pt(3)–P(2)	2.229(5)
Pt(3)–I	2.6466(15)		
C(1)–Pt(1)–C(1')	86.7(10)	C(1)–Pt(1)–P(1')	164.8(5)
C(1)–Pt(1)–P(1)	84.9(5)	P(1')–Pt(1)–P(1)	105.9(2)
P(1)–Pt(2)–P(1')	104.7(2)	P(1)–Pt(2)–P(2')	148.89(15)
P(1)–Pt(2)–P(2)	97.3(2)	P(2')–Pt(2)–P(2)	72.9(2)
P(2)–Pt(3)–P(2')	78.7(2)	P(2)–Pt(3)–I'	94.12(12)
P(2)–Pt(3)–I	172.85(12)	I'–Pt(3)–I	93.03(8)
Pt(1)–P(1)–Pt(2)	74.70(14)	Pt(3)–P(2)–Pt(2)	104.2(2)

^a Symmetry transformation used to generate equivalent primed atoms: *x*, *y*, *−z* + 3/2.

molar ratio) proceeds with different results, depending on the reaction conditions. Thus, when the reaction is carried out at 213 K and with a very short reaction time (10 min), the trinuclear platinum complex, in mixed oxidation state Pt(III)–Pt(III)–Pt(II), $[(\text{R}_f)_2\text{Pt}(\mu\text{-PPh}_2)_2\text{Pt}(\mu\text{-PPh}_2)_2\text{PtI}_2]$ **11** is obtained. This 46 VEC complex has to display a Pt–Pt bond, which can be located at two different positions, and because of that, an XRD study has been carried out. This, which will be discussed in detail later, reveals that the Pt–Pt bond is located between the central Pt atom and the one containing the C₆F₅ groups. This is an important fact, which allows for explanation of the evolution of **11** at room temperature. The formation of **11** is not surprising and seems to be the result of the oxidation of **10** to form a mixed Pt(III)–Pt(III)–Pt(II) complex and substitution of the labile acetonitrile by the formed I[−]. We have observed, previously, similar behavior with other similar binuclear derivatives.¹⁹

On the other hand, when a CH₂Cl₂ solution of **10** is treated with a CH₂Cl₂ solution of I₂ (1:1 molar ratio) and the mixture is stirred at room temperature for 24 h, a yellow solid identified as **8** (Scheme 1) is obtained. Obviously, the formation of **8** is again a consequence of the transformation of **11**, which at room temperature results in a PPh₂/C₆F₅ reductive coupling. This is an already-known process which takes place in pentafluorophenyl binuclear platinum complexes.¹⁹

The crystal structure of complex **11** has been determined by single-crystal X-ray diffraction. (Figure 8, Table 6). Complex **11** is a trinuclear complex in which, and in accordance with

the crystallographic symmetry on the molecule, the three Pt atoms form a straight line. The phosphido ligands bridge the Pt centers, the coordination of the external platinum atoms being completed by two terminal pentafluorophenyl groups, attached to Pt(1), and two terminal iodo ligands bonded to Pt(3). The Pt(1)–Pt(2) distance is short, 2.778(1) Å, indicating the existence of a Pt–Pt bond, while no interaction is present between Pt(2) and Pt(3) (distance 3.636(1) Å). In accordance with the existence of the Pt(1)–Pt(2) bond, the P(1)–Pt(1,2)–P(1') angles are broad and the Pt(1)–P(1,1')–Pt(2) angles are narrow (see Table 6). The continuous shape measures²⁶ obtained for Pt(1), $S(SP-4) = 2.037$, and Pt(3), $S(SP-4) = 1.172$, indicate that these atoms lie in the centers of square-planar environments. Nevertheless, Pt(2) shows a significant deviation from the $SP-4$ geometry, as is evident in the value of the continuous shape measure: $S(SP-4) = 6.490$.²⁶ Thus, the planes formed by the Pt(2), P(1), and P(1') atoms and the Pt(2), P(2), and P(2') atoms are rotated one with respect to the other and form a dihedral angle of 39.1(1)°. Thus, the core of complex **11** can be regarded as formed by two planes “C₂Pt(1)(μ-P)₂Pt(2)” and “Pt(2)(μ-P)₂Pt(3)I₂” rotated one with respect to the other, with the Pt(2) center as a pivot point.

The ¹⁹F NMR spectrum of **11** registered at room temperature shows the expected pattern for the proposed structure: three signals in a 2:1:2 intensity ratio. Moreover, some signals of very low intensity assigned to the hexanuclear complex **8** are also observed. The ³¹P{¹H} NMR spectrum of **11** at 183 K shows only two signals at δ 261.9 and –157.1, in agreement with the presence of two “Pt(μ-PPh₂)₂Pt” fragments with and without a metal–metal bond, respectively, as expected for **11**. The signals are broad, and from the spectrum, only the coupling constants with the ¹⁹⁵Pt atoms can be extracted. When the same spectrum is recorded at room temperature, the signals indicate now the existence in solution of a mixture made up of the hexanuclear complex **8** as the main component and a very small amount of the trinuclear complex **11**. These results indicate that **11** is unstable in solution at room temperature and evolves toward **8** through the coupling of the PPh₂ and C₆F₅ groups bonded to a Pt(III) center. The evolution of **11** to **8** can be compared with the evolution of the binuclear platinum(III) complex [(R_F)₂Pt(μ-PPh₂)₂PtI₂], which renders the tetranuclear platinum(II) [(R_F)Pt(μ-PPh₂)(μ-I)Pt(PPh₂R_F)(μ-I)]₂. It is obvious that the reductive coupling process, which transforms **11** into **8**, takes place between ligands bonded to metal centers in a formal +3 oxidation state.

(26) For the definition and use of the continuous shape measure, S , as a parameter quantifying the reliability with which a real coordination entity can be described by means of a given regular geometric polyhedron, see: (a) Pinsky, M.; Avnir, D. *Inorg. Chem.* **1998**, *37*, 5575. (b) Casanova, D.; Llunell, M.; Alemany, P.; Alvarez, S. *Chem.–Eur. J.* **2005**, *11*, 1479. (c) Cirera, J.; Alemany, P.; Alvarez, S. *Chem.–Eur. J.* **2004**, *10*, 190. (d) Casanova, D.; Alemany, P.; Bofill, J. M.; Alvarez, S. *Chem.–Eur. J.* **2003**, *9*, 281. (e) Alvarez, S.; Avnir, D.; Llunell, M.; Pinsky, M. *New J. Chem.* **2002**, 996. (f) Alvarez, S.; Llunell, M. *J. Chem. Soc., Dalton Trans.* **2000**, 3288. The smaller the value of S , the better the agreement between the real molecule and the suggested model, $S = 0$ being for perfect coincidence.

Concluding Remarks

The oxidative addition of X₂ (X = halogen) to square-planar d⁸ platinum(II) centers usually affords Pt(IV) complexes,^{27–30} and the addition to binuclear derivatives is an entry to binuclear Pt(III) derivatives. The metal centers in the binuclear Pt(III) complexes usually display an octahedral environment.^{31–35} The addition of I₂ to our polynuclear phosphido derivatives of platinum(II) is carried out with two-electron oxidation on a Pt₂(II) unit, giving a Pt₂(III) unit. Nevertheless, in our phosphido Pt₂(III) fragments, the two metal centers display nearly coplanar square-planar coordination environments. The complexes are not stable enough, and they evolve to new polynuclear Pt(II) derivatives.

The oxidative addition-reductive coupling (with or without elimination) sequences,^{36–41} involving M(0)/M(II)/M(0) or M(II)/M(IV)/M(II) (M = palladium or platinum), have been proposed in a great number of reaction processes. In our case, these sequences involve Pt₂(II)/Pt₂(III)/Pt₂(II) fragments, the Pt(III) intermediates being isolated.

The activation of a P–C bond of a tertiary phosphine is an easy entry into phosphido complexes of transition metals.^{42–50} The reverse M–P and M–C cleavage and P–C bond formation in phosphido derivatives is unusual, but it has been observed in some cases.^{4,18,19,21,51–53} This P–C coupling is even more remarkable taking into consideration the strength of the Pt–C₆F₅ and Pt–PPh₂ bonds in the

- (27) Yahav, A.; Goldberg, I.; Vignalok, A. *Organometallics* **2005**, *24*, 5654–5659.
- (28) Gracia, C.; Marco, G.; Navarro, R.; Romero, P.; Soler, T.; Urriolabeitia, E. P. *Organometallics* **2003**, *22*, 4910–4921.
- (29) Fornies, J.; Fortuño, C.; Gómez, M. A.; Menjón, B. *Organometallics* **1993**, *12*, 4368–4375.
- (30) Ruiz, J.; López, J. F. J.; Rodríguez, V.; Pérez, J.; Ramírez de Arellano, M. C.; López, G. *J. Chem. Soc., Dalton Trans.* **2001**, 268, 3–2689.
- (31) Bennett, M. A.; Bhargava, S. K. M. B. A.; Edwards, A. J.; Guo, S.-X.; Privér, S. H.; Rae, A. D.; Willis, A. C. *Inorg. Chem.* **2004**, *43*, 7752–7763.
- (32) Matsumoto, K.; Ochiai, M. *Coord. Chem. Rev.* **2002**, *231*, 229–238.
- (33) Rendina, L. M.; Hambley, T. W. In *Comprehensive Coordination Chemistry II*; McCleverty, J. A., Meyer, T. J. Eds.; Elsevier Inc.: San Diego, 2004; Vol. 6.
- (34) Lippert, B. *Coord. Chem. Rev.* **1999**, 263–295.
- (35) Muller, J.; Freisinger, E.; Sanz-Miguel, P. J.; Lippert, B. *Inorg. Chem.* **2003**, *42*, 5117–5125.
- (36) van Belzen, R.; Elsevier, C. J.; Dedieu, A.; Veldman, N.; Spek, A. L. *Organometallics* **2003**, *22*, 722–736.
- (37) Christmann, U.; Vilar, R. *Angew. Chem., Int. Ed.* **2005**, *44*, 366–374.
- (38) Leca, F.; Sauthier, M.; Deborde, V.; Toupet, L.; Réau, R. *Chem.–Eur. J.* **2003**, *9*, 3785–3795.
- (39) Moncarz, J. R.; Brunker, T. J.; Glueck, D. S.; Sommer, R. D.; Rheingold, A. L. *J. Am. Chem. Soc.* **2003**, *125*, 1180–1181.
- (40) Hristov, I. H.; Ziegler, T. *Organometallics* **2003**, *22*, 3513–3525.
- (41) Espinet, P.; Echavarran, A. M. *Angew. Chem., Int. Ed.* **2004**, *42*, 4704–4734.
- (42) Zhuravel, M. A.; Moncarz, J. R.; Glueck, D. S.; Lam, K.-C.; Rheingold, A. L. *Organometallics* **2000**, *19*, 3447–3454.
- (43) Shulman, P. M.; Burkhardt, E. D.; Lundquist, E.; Pilato, R. S.; Geoffroy, G. L.; Rheingold, A. L. *Organometallics* **1987**, *6*, 101–109.
- (44) Mizuta, T.; Onishi, M.; Nakazono, T.; Nakazawa, H.; Miyoshi, K. *Organometallics* **2002**, *21*, 717–726.
- (45) Bender, R.; Braunstein, P.; Dedieu, A.; Ellis, P. D.; Huggins, B.; Harvey, P. D.; Sappa, E.; Tiripicchio, A. *Inorg. Chem.* **1996**, *35*, 1223–1234.
- (46) Shiu, K. B.; Jean, S. W.; Wang, S. L.; Liao, F. L.; Wang, J. C.; Liou, L. S. *Organometallics* **1997**, *16*, 114–119.
- (47) García, G.; García, M. E.; Melón, S.; Riera, V.; Ruiz, M. A.; Villafañe, F. *Organometallics* **1997**, *16*, 624–631.

precursors, and with no doubt the +3 oxidation state of the Pt center, in a nonoctahedral environment, plays a key role in this process.

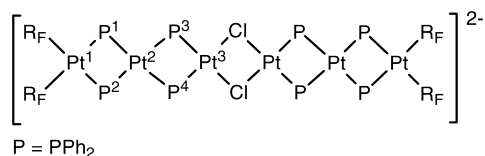
From the spectroscopic point of view, Pt atoms in the +3 oxidation state and in a nonoctahedral environment exhibit strong *shielding* of their ^{195}Pt nuclei with respect to their Pt(II) precursors, as ascertained by $^{195}\text{Pt}\{^1\text{H}\}$ and $^{19}\text{F}-^{195}\text{Pt}$ HMQC experiments. The fact that ^{195}Pt (III) nuclei in octahedral environments experience a *deshielding* with respect to their Pt(II) precursors suggests that the presence of three-membered Pt₂P rings may play a role for such effects.

Experimental Section

General Comments. Literature methods were used to prepare the starting material $[\text{NBu}_4][(\text{R}_\text{F})_2\text{Pt}(\mu\text{-PPh}_2)_2\text{Pt}(\mu\text{-PPh}_2)_2\text{Pt}(\text{R}_\text{F})_2]$.³ C, H, and N analysis and IR spectra procurement were performed as described elsewhere.¹⁹ NMR spectra were recorded on Bruker ARX 300, Varian UNITY 300, and Bruker Avance 400 spectrometers; frequencies are referenced to SiMe_4 (^1H), CFCl_3 (^{19}F), 85% H_3PO_4 (^{31}P), and H_2PtCl_6 (^{195}Pt). NMR simulations were performed using the program WINDAISY 4.05. Signal attributions and coupling constant assessments were made on the basis of a multinuclear NMR analysis that included $^{19}\text{F}-^{31}\text{P}$ HMQC, $^{19}\text{F}-^{195}\text{Pt}$ HMQC, and $^{31}\text{P}\{^1\text{H}\}$ COSY experiments. Coupling constants not directly extractable from the 1D spectra were obtained and attributed on the basis of the tilts of the multiplets due to the “passive” nuclei⁵⁴ in the aforementioned 2D spectra.

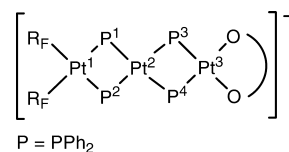
Caution! *Perchlorate salts of metal complexes with organic ligands are potentially explosive. Only small amounts of materials should be prepared, and these should be handled with great caution.*

Synthesis of $[\text{NBu}_4][(\text{R}_\text{F})_2\text{Pt}(\mu\text{-PPh}_2)_2\text{Pt}(\mu\text{-PPh}_2)_2\text{Pt}(\mu\text{-Cl})_2]$, **4.** To a yellow solution of **1** (2.000 g, 0.800 mmol) in acetone (30 mL) was added HCl (1.600 mmol, HCl/H₂O solution, 0.24 M). The solution was stirred for 20 h and evaporated to ca. 2 mL. $^i\text{PrOH}$ (20 mL) was added, and the mixture was stirred for 5 h. The yellow solid **4** was filtered off, washed with $^i\text{PrOH}$ (3 × 1 mL), and vacuum-dried (1.330 g, 85% yield). Anal. found (calcd for $\text{C}_{152}\text{Cl}_2\text{F}_{20}\text{H}_{152}\text{N}_2\text{P}_8\text{Pt}_6$): C, 46.97 (47.07); H, 3.82 (3.92); N, 0.60 (0.72). IR (cm^{-1}): 779, 771 (X-sensitive C_6F_5). $\Lambda_{\text{M}} = 84 \text{ ohm}^{-1} \text{ cm}^2 \text{ mol}^{-1}$. ^{19}F NMR (acetone- d_6 , 295 K): $\delta -113.8$ (*o*-F, d, $^3J_{\text{F,F}} = 30 \text{ Hz}$, $^3J_{\text{F,Pt(1)}} = 324 \text{ Hz}$), -167.6 (*m*-F, br m), -168.9 (*p*-F, t, $^3J_{\text{F,F}} = 20 \text{ Hz}$). $^{31}\text{P}\{^1\text{H}\}$ NMR (acetone- d_6 , 295 K): $\delta -111.6$ [P(1/2), m], $^2J_{\text{P(1),P(2)}} = 125 \text{ Hz}$, $^2J_{\text{P(1),P(3)}} = 13 \text{ Hz}$, $^2J_{\text{P(1),P(4)}} = 293 \text{ Hz}$, $^1J_{\text{P(1),Pt(1)}} = 1771 \text{ Hz}$, $^1J_{\text{P(1),Pt(2)}} = 1624 \text{ Hz}$], -128.4 [P(3/4), m], $^2J_{\text{P(3),P(1)}} = 13 \text{ Hz}$, $^2J_{\text{P(3),P(2)}} = 293 \text{ Hz}$, $^2J_{\text{P(3),P(4)}} = 163 \text{ Hz}$, $^1J_{\text{P(3),Pt(2)}} = 1714 \text{ Hz}$, $^1J_{\text{P(3),Pt(3)}} = 2552 \text{ Hz}$]. $^{195}\text{Pt}\{^1\text{H}\}$ NMR (acetone- d_6 , 295 K): $\delta -3337$ [Pt(3), t], $^1J_{\text{Pt(3),P(3)}} = 2552 \text{ Hz}$], -3795 [Pt(1), m], $^1J_{\text{Pt(1),Pt(1)}} = 1771 \text{ Hz}$], -3857 [Pt(2), tt], $^1J_{\text{Pt(2),Pt(1)}} = 1624 \text{ Hz}$, $^1J_{\text{Pt(2),P(3)}} = 1714 \text{ Hz}$].



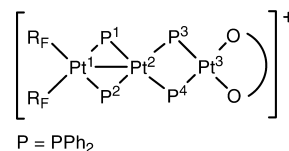
Synthesis of $[\text{NBu}_4][(\text{R}_\text{F})_2\text{Pt}(\mu\text{-PPh}_2)_2\text{Pt}(\mu\text{-PPh}_2)_2\text{Pt}(\text{acac})]$, **5.** To a yellow solution of **4** (0.704 g, 0.181 mmol) in acetone (30 mL) was added Tlacac (0.116 g, 0.381 mmol). The mixture was stirred in the dark for 20 h and filtered through celite. The solution was evaporated to ca. 2 mL; $^i\text{PrOH}$ (20 mL) was added, and the mixture was stirred for 3 h. The yellow solid **5** was filtered off,

washed with $^i\text{PrOH}$ (2 × 0.5 mL), and vacuum-dried (0.534 g, 73% yield). Anal. found (calcd for $\text{C}_{81}\text{F}_{10}\text{H}_{83}\text{NO}_2\text{P}_4\text{Pt}_3$): C, 48.56 (48.53); H, 3.47 (4.18); N, 0.55 (0.70). IR (cm^{-1}): 778, 769 (X-sensitive C_6F_5); 1562, 1515 ($\nu(\text{C}=\text{C})$, $\nu(\text{C}=\text{O})$ acac). $\Lambda_{\text{M}} = 51 \text{ ohm}^{-1} \text{ cm}^2 \text{ mol}^{-1}$. ^{19}F NMR (acetone- d_6 , 295 K): $\delta -113.1$ (*o*-F, d, $^3J_{\text{F,F}} = 30 \text{ Hz}$, $^3J_{\text{F,Pt(1)}} = 329 \text{ Hz}$), -167.6 (*m*-F, br m), -168.9 (*p*-F, t, $^3J_{\text{F,F}} = 20 \text{ Hz}$). $^{31}\text{P}\{^1\text{H}\}$ NMR (acetone- d_6 , 295 K): $\delta -113.0$ [P(1/2), $^2J_{\text{P(1),P(2)}} = 150 \text{ Hz}$, $^2J_{\text{P(1),P(3)}} = 7 \text{ Hz}$, $^2J_{\text{P(1),P(4)}} = 298 \text{ Hz}$, $^1J_{\text{P(1),Pt(1)}} = 1769 \text{ Hz}$, $^1J_{\text{P(1),Pt(2)}} = 1626 \text{ Hz}$, $^3J_{\text{P(1),Pt(3)}} = 77 \text{ Hz}$], -132.5 [P(3/4), $^2J_{\text{P(3),P(1)}} = 7 \text{ Hz}$, $^2J_{\text{P(3),P(2)}} = 298 \text{ Hz}$, $^2J_{\text{P(3),P(4)}} = 117 \text{ Hz}$, $^1J_{\text{P(3),Pt(2)}} = 1730 \text{ Hz}$, $^1J_{\text{P(3),Pt(3)}} = 2590 \text{ Hz}$]. $^{195}\text{Pt}\{^1\text{H}\}$ NMR (acetone- d_6 , 295 K): $\delta -3159$ [Pt(3), t, $^1J_{\text{Pt(3),P(3)}} = 2590 \text{ Hz}$], -3793 [Pt(1), m, $^1J_{\text{Pt(1),Pt(1)}} = 1769 \text{ Hz}$], -3894 [Pt(2), tt, $^1J_{\text{Pt(2),Pt(1)}} = 1626 \text{ Hz}$, $^1J_{\text{Pt(2),P(3)}} = 1730 \text{ Hz}$].



Reaction of $[\text{NBu}_4][(\text{R}_\text{F})_2\text{Pt}(\mu\text{-PPh}_2)_2\text{Pt}(\mu\text{-PPh}_2)_2\text{Pt}(\text{acac})]$, **5, with HCl.** To a yellow solution of **5** (0.150 g, 0.075 mmol) in acetone (10 mL) was added 0.32 mL (0.075 mmol) of HCl (HCl/H₂O, 0.24 M). The solution was stirred for 24 h and evaporated to ca. 1 mL, and $^i\text{PrOH}$ (10 mL) was added. Complex **4** crystallizes upon stirring, which was filtered off and washed with $^i\text{PrOH}$ (2 × 1 mL) and vacuum-dried (0.072 g, 50% yield).

Synthesis of $[(\text{R}_\text{F})_2\text{Pt}(\mu\text{-PPh}_2)_2\text{Pt}(\mu\text{-PPh}_2)_2\text{Pt}(\text{acac})][\text{ClO}_4]$, **6.** To a yellow solution of **5** (0.270 g, 0.135 mmol) in CH_2Cl_2 (20 mL) was added AgClO_4 (0.060 g, 0.289 mmol). The mixture was stirred in the dark for 7 h and filtered through celite. The orange solution was evaporated to ca. 2 mL, and $^i\text{PrOH}$ (3 mL) was added. The solution was evaporated until an orange solid crystallized, **6**, which was filtered off, washed with cold $^i\text{PrOH}$ (2 × 0.5 mL), and vacuum-dried (0.142 g, 57% yield). Anal. found (calcd for $\text{C}_{65}\text{ClF}_{10}\text{H}_{47}\text{O}_6\text{P}_4\text{Pt}_3$): C, 41.63 (41.98); H, 1.99 (2.54). IR (cm^{-1}): 794, 784 (X-sensitive C_6F_5); 1561, 1522 ($\nu(\text{C}=\text{C})$, $\nu(\text{C}=\text{O})$ acac). $\Lambda_{\text{M}} = 86 \text{ ohm}^{-1} \text{ cm}^2 \text{ mol}^{-1}$. ^{19}F NMR (CDCl_3 , 295 K): $\delta -119.5$ (*o*-F, d, $^3J_{\text{F,F}} = 23 \text{ Hz}$, $^3J_{\text{F,Pt(1)}} = 280 \text{ Hz}$), -156.2 (*p*-F, t, $^3J_{\text{F,F}} = 20 \text{ Hz}$), -160.7 (*m*-F, br m). $^{31}\text{P}\{^1\text{H}\}$ NMR (CDCl_3 , 295 K): $\delta 268.6$ [P(1/2), $^2J_{\text{P(1),P(2)}} = 40.1 \text{ Hz}$, $^2J_{\text{P(1),P(3)}} = 24 \text{ Hz}$, $^2J_{\text{P(1),P(4)}} = 114 \text{ Hz}$, $^1J_{\text{P(1),Pt(1)}} = 1305 \text{ Hz}$, $^1J_{\text{P(1),Pt(2)}} = 1065 \text{ Hz}$, $^3J_{\text{P(1),Pt(3)}} = 50 \text{ Hz}$], -137 [P(3/4), $^2J_{\text{P(3),P(1)}} = 24 \text{ Hz}$, $^2J_{\text{P(3),P(2)}} = 114 \text{ Hz}$, $^2J_{\text{P(3),P(4)}} = 107 \text{ Hz}$, $J_{\text{P(3),Pt(1)}} = 80 \text{ Hz}$, $^1J_{\text{P(3),Pt(2)}} = 1939 \text{ Hz}$, $^1J_{\text{P(3),Pt(3)}} = 2967 \text{ Hz}$]. $^{195}\text{Pt}\{^1\text{H}\}$ NMR (CDCl_3 , 295K): $\delta -3087$ [Pt(3), t, $^1J_{\text{Pt(3),P(3)}} = 2967 \text{ Hz}$], -3793 [Pt(1), m, $^1J_{\text{Pt(1),Pt(1)}} = 1305 \text{ Hz}$, $^1J_{\text{Pt(1),Pt(2)}} = 434 \text{ Hz}$], -3894 [Pt(2), tt, $^1J_{\text{Pt(2),Pt(1)}} = 1065 \text{ Hz}$, $^1J_{\text{Pt(2),P(3)}} = 1939 \text{ Hz}$, $^1J_{\text{Pt(2),Pt(1)}} = 434 \text{ Hz}$].



Reaction of $[(\text{R}_\text{F})_2\text{Pt}(\mu\text{-PPh}_2)_2\text{Pt}(\mu\text{-PPh}_2)_2\text{Pt}(\text{acac})][\text{ClO}_4]$ with NBu_4BH_4 . To an orange solution of **6** (0.100 g, 0.054 mmol) in CH_2Cl_2 (10 mL) was added NBu_4BH_4 (0.030 g, 0.116 mmol) solved in methanol (2 mL). The yellow solution was evaporated to ca. 1 mL; $^i\text{PrOH}$ (10 mL) was added, and **5** crystallized (0.042 g, 41% yield).

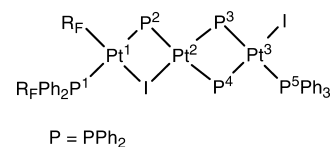
Reaction of $[(\text{R}_\text{F})_2\text{Pt}(\mu\text{-PPh}_2)_2\text{Pt}(\mu\text{-PPh}_2)_2\text{Pt}(\text{acac})][\text{ClO}_4]$ with NBu_4Br . To an orange solution of **6** (0.350 g, 0.188 mmol) in CH_2Cl_2 (20 mL) was added NBu_4Br (0.061 g, 0.189 mmol). The

solution was stirred for 68 h and evaporated to dryness. Et₂O (20 mL) was added to the residue, and a white solid (NBu₄ClO₄) was filtered off. The solution was evaporated to ca. 2 mL, and hexane (20 mL) was added. A yellow solid crystallized that was filtered, washed with hexane (2 × 0.5 mL), and vacuum-dried (0.149 g, 57% yield, **7a/7b** ratio ca. 3.5:1). The solution was left in the freezer for 3 days, and a second fraction of yellow solid crystallized that was filtered, washed with cold hexane (2 × 0.5 mL), and vacuum-dried (0.031 g, 9% yield, **7a/7b** ratio ca. 1:2.9). Anal. found (calcd for BrC₆₅F₁₀H₄₇O₂P₄Pt₃): C, 42.33 (42.45); H, 2.73 (2.57). IR (cm⁻¹): 1520, 983 (PPh₂C₆F₅); 802 **7a**, 784 **7b** (X-sensitive C₆F₅); 1575, 1520 (ν(C=C), ν(C=O) acac). ¹H NMR (CDCl₃, 293 K) for **7a** and **7b**: δ 5.2 (CH, acac), 1.7 (CH₃, acac), 1.6 (CH₃, acac). ¹⁹F NMR (CDCl₃, 293 K) for **7a**: δ -117.7 (2 *o*-F, ³J_{F,Pt(1)}} = 449 Hz), -124.5 (2 *o*-F, PPh₂C₆F₅), -148.7 (1 *p*-F, PPh₂C₆F₅), -160.7 (2 *m*-F, PPh₂C₆F₅), -164.5 (1 *p*-F), -165.5 (2 *m*-F). For **7b**: δ -119.2 (2 *o*-F, ³J_{F,Pt(1)}} = 221 Hz), -122.1 (2 *o*-F, PPh₂C₆F₅), -147.7 (1 *p*-F, PPh₂C₆F₅), -160.4 (2 *m*-F, PPh₂C₆F₅), -161.8 (1 *p*-F), -163.7 (2 *m*-F). ³¹P{¹H} NMR (CDCl₃, 293 K) for **7a**: δ 15.3 [P2, d, ²J_{P(1),P(2)}} = 333 Hz, ¹J_{P(2),Pt(1)}} = 2307 Hz], -31.3 [P1, dd, ²J_{P(1),P(2)}} = 333 Hz, ²J_{P(1),P(4)}} = 306 Hz, ¹J_{P(1),Pt}} = 1965, 1764 Hz], -134.0 [P3, d, ²J_{P(3),P(4)}} = 170 Hz, ¹J_{P(3),Pt}} = 3001, 3265 Hz], -146.0 [P4, dd, ²J_{P(1),P(4)}} = 306 Hz, ²J_{P(3),P(4)}} = 170 Hz, ¹J_{P(4),Pt(2)}} = 1770 Hz, ¹J_{P(4),Pt(3)}} = 2015 Hz]. For **7b**: δ -5.0 [P2, s, ¹J_{P(2),Pt(1)}} = 4861 Hz], -37.9 [P1, d, ²J_{P(1),P(4)}} = 295 Hz, ¹J_{P(1),Pt(1)}} ≈ ¹J_{P(1),Pt(2)}} ≈ 1600 Hz], -132.9 [P3, d, ²J_{P(3),P(4)}} = 173 Hz, ¹J_{P(3),Pt}} = 2964, 3390 Hz], -146.5 [P4, dd, ²J_{P(1),P(4)}} = 295 Hz, ²J_{P(3),P(4)}} = 173 Hz, ¹J_{P(4),Pt(2)}} = 1720 Hz, ¹J_{P(4),Pt(3)}} = 2656 Hz].

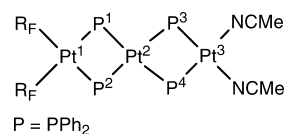
Reaction of [NBu₄][(R_F)₂Pt(μ-PPh₂)₂Pt(μ-PPh₂)₂Pt(acac)] with I₂. To a solution of **5** (0.200 g, 0.100 mmol) in CH₂Cl₂ (15 mL) was dripped a CH₂Cl₂ solution (10 mL) of I₂ (0.026 g, 0.100 mmol). The solution was stirred for 30 h and evaporated to ca. 2 mL, and ⁱPrOH (10 mL) was added. A yellow solid, **8**, crystallized, which was filtered, washed with ⁱPrOH (2 × 0.5 mL), and vacuum-dried (0.085 g, 44% yield). Anal. found (calcd for C₁₂₀F₂₀H₈₀I₄P₈Pt₆): C, 37.60 (37.62); H, 1.90 (2.09). IR (cm⁻¹): 1519, 982 (PPh₂C₆F₅); 801 (X-sensitive C₆F₅). ¹⁹F NMR (acetone-d₆, 293 K): δ -116.4 (2 *o*-F, ³J_{F,Pt(1)}} = 440 Hz), -124.0 (2 *o*-F, PPh₂C₆F₅), -150.0 (1 *p*-F, PPh₂C₆F₅), -161.8 (2 *m*-F, PPh₂C₆F₅), -164.8 (1 *p*-F), -165.1 (2 *m*-F). ³¹P{¹H} NMR (acetone-d₆, 293 K): δ 12.9 [P1, d, ²J_{P(1),P(2)}} = 332 Hz, ¹J_{P1,Pt(1)}} = 2303 Hz], -44.6 [P2, dd, ²J_{P(1),P(2)}} = 332 Hz, ²J_{P(2),P(4)}} = 303 Hz, ¹J_{P(2),Pt(1)}} ≈ ¹J_{P(2),Pt(1)}} ≈ 1870 Hz], -142.6 [P3, d, ²J_{P(3),P(4)}} = 175 Hz, ¹J_{P(3),Pt}} = 3154, 2806 Hz], -152.6 [P4, dd, ²J_{P(2),P(4)}} = 303 Hz, ²J_{P(3),P(4)}} = 175 Hz, ¹J_{P(4),Pt}} can not be measured unambiguously].

Reaction of [(PPh₂R_F)(R_F)Pt(μ-PPh₂)(μ-I)Pt(μ-PPh₂)₂Pt(μ-D)]₂ with PPh₃. To a yellow suspension of **8** (0.114 g, 0.029 mmol) in acetone (20 mL) was added PPh₃ (0.016 g, 0.060 mmol), and this was stirred for 24 h. The mixture was filtered through celite, and the solution was evaporated to ca. 0.5 mL. CHCl₃ (2 mL) was added, and a yellow solid, **9**, crystallized, which was filtered, washed with cold CHCl₃ (2 × 0.5 mL), and vacuum-dried (0.025 g, 19% yield). Anal. found (calcd for C₇₈F₁₀H₅₅I₂P₅Pt₃): C, 42.96 (43.02);

H, 2.13 (2.52). IR (cm⁻¹): 1519, 982 (PPh₂C₆F₅); 798 (X-sensitive C₆F₅). ¹⁹F NMR (CD₂Cl₂, 293 K): δ -117.6 (2 *o*-F, ³J_{F,Pt}} = 432 Hz), -124.2 (2 *o*-F, PPh₂C₆F₅), -149.1 (1 *p*-F, PPh₂C₆F₅), -161.0 (2 *m*-F, PPh₂C₆F₅), -165.0 (1 *p*-F), -165.3 (2 *m*-F). ³¹P{¹H} NMR (CD₂Cl₂, 293 K): δ 20.0 [P5, d, ²J_{P(5),P(3)}} = 392 Hz, ¹J_{P(5),Pt(3)}} = 2154 Hz], 12.9 [P1, d, ²J_{P(1),P(2)}} = 329 Hz, ¹J_{P(1),Pt(1)}} = 2283 Hz], -40.8 [P2, dd, ²J_{P(2),P(1)}} = 329 Hz, ²J_{P(2),P(4)}} = 304 Hz, ¹J_{P(2),Pt(1)}} = 1677 Hz, ¹J_{P(2),Pt(2)}} = 1854 Hz], -148.7 [P3, dd, ²J_{P(3),P(4)}} = 190 Hz, ²J_{P(3),P(5)}} = 392 Hz, ¹J_{P(3),Pt(2)}} = 2863, ¹J_{P(3),Pt(3)}} = 1846 Hz], -162.2 [P4, dd, ²J_{P(4),P(2)}} = 304 Hz, ²J_{P(4),P(3)}} = 190 Hz, ¹J_{P(4),Pt(2)}} = 1561 Hz, ¹J_{P(4),Pt(3)}} = 2509 Hz]. ¹⁹⁵Pt{¹H} NMR (CD₂Cl₂, 295 K): δ -3959 [Pt(2), ddd, ¹J_{Pt(2),P(2)}} = 1854 Hz, ¹J_{Pt(2),P(3)}} = 2863 Hz, ¹J_{Pt(2),P(4)}} = 1561 Hz], -4416 [Pt(3), ddd, ¹J_{Pt(3),P(3)}} = 1846 Hz, ¹J_{Pt(3),P(4)}} = 2509 Hz, ¹J_{Pt(3),P(5)}} = 2154 Hz], -4525 [Pt(1), dd, ¹J_{Pt(1),P(1)}} = 2283 Hz, ¹J_{Pt(1),P(2)}} = 1677 Hz].



Synthesis of [(R_F)₂Pt(μ-PPh₂)₂Pt(μ-PPh₂)₂Pt(NCMe)₂], 10. To a yellow solution of **5** (1.000 g, 0.499 mmol) in MeCN (15 mL) was added HClO₄ (0.499 mmol, 2.85 mL of a HClO₄/MeOH solution at 0.175 M). Instantaneously, a pale yellow solid crystallized, **10**, which was stirred for 30 min, filtered, washed with cold MeCN (2 × 0.5 mL), and vacuum-dried (0.761 g, 87% yield). Anal. found (calcd for C₆₄F₁₀H₄₆N₂P₄Pt₃): C, 43.88 (44.09); H, 2.43 (2.64); N, 1.64 (1.60). IR (cm⁻¹): 2323, 2316 (ν(C≡N)); 782, 770 (X-sensitive C₆F₅). ¹⁹F NMR (DMF, 295 K): δ -113.5 (*o*-F, d, ³J_{F,F}} = 30 Hz, ³J_{F,Pt(1)}} = 317 Hz), -166.7 (*m*-F, br m), -167.4 (*p*-F, t, ³J_{F,F}} = 20 Hz). ³¹P{¹H} NMR (DMF, 315 K): δ -118.8 [P(1/2), ¹J_{P(1),P(2)}} = 150 Hz, ¹J_{P(1),P(3)}} = 3 Hz, ¹J_{P(1),P(4)}} = 298 Hz, ¹J_{P(1),Pt(1)}} = 1740 Hz, ¹J_{P(1),Pt(2)}} = 1670 Hz], -128.8 [P(3/4), ¹J_{P(3),P(1)}} = 3 Hz, ¹J_{P(3),P(2)}} = 298 Hz, ¹J_{P(3),P(4)}} = 120 Hz, ¹J_{P(3),Pt(2)}} = 1700 Hz, ¹J_{P(3),Pt(3)}} = 2690 Hz]. ¹⁹⁵Pt{¹H} NMR (dmf, 295 K): δ -3461 [Pt(3), t, ¹J_{Pt(3),P(3)}} = 2690 Hz], -3773 [Pt(1), m, ¹J_{Pt(1),Pt(1)}} = 1740 Hz], -3881 [Pt(2), tt, ¹J_{Pt(2),P(1)}} = 1670 Hz, ¹J_{Pt(2),P(3)}} = 1700 Hz].



Reaction of [(R_F)₂Pt(μ-PPh₂)₂Pt(μ-PPh₂)₂Pt(NCMe)₂] with I₂. To a pale yellow suspension of **10** (0.150 g, 0.086 mmol) in CH₂Cl₂/MeCN (20/5 mL) was dropped I₂ (0.022 g, 0.086 mmol) in CH₂Cl₂ (5 mL). The mixture was stirred for 24 h at room temperature, and the solution was evaporated to ca. 1 mL. A yellow solid crystallized, **8**, which was filtered and vacuum-dried (0.084 g, 51% yield).

To a pale yellow suspension of **10** (0.150 g, 0.086 mmol) in CH₂Cl₂/MeCN (20/5 mL) at 213 K was dropped I₂ (0.022 g, 0.086 mmol) in CH₂Cl₂ (5 mL). The mixture was stirred at 213 K for 10 min, and a small amount of yellow solid was filtered off. The dark red solution was evaporated to ca. 1 mL, and hexane (20 mL) was added. The brown-red solid, **11**, was filtered, washed with hexane (2 × 1 mL), and vacuum-dried (0.113 g, 66% yield). Anal. found (calcd for C₆₀F₁₀H₄₀I₂P₄Pt₃): C, 37.26 (37.63); H, 2.06 (2.09). IR (cm⁻¹): 794, 782 (X-sensitive C₆F₅). ¹⁹F NMR (CD₂Cl₂, 293 K): δ -118.3 (*o*-F, ³J_{F,Pt(1)}} = 288 Hz), -157.0 (*p*-F), -161.4 (*m*-F). ³¹P{¹H} NMR (CD₂Cl₂, 183 K): δ 261.9 (P atoms trans to C₆F₅, ¹J_{P,Pt}} = 1198, 1325 Hz), -157.1 (P atoms trans to I, ¹J_{P,Pt}} = 1664, 2709 Hz).

- (48) Fahey, D. R.; Mahan, J. E. *J. Am. Chem. Soc.* **1976**, *98*, 4499–4503.
 (49) Ang, H. G.; Kwik, W. L.; Leong, W. K.; Johnson, B. F. G.; Lewis, J.; Raithby, P. R. *J. Organomet. Chem.* **1990**, *396*, C43.
 (50) Heyn, R. H.; Gorbitz, C. H. *Organometallics* **2002**, *21*, 2781–2784.
 (51) Archambault, C.; Bender, R.; Braunstein, P.; Decian, A.; Fischer, J. *Chem. Commun.* **1996**, 2729–2730.
 (52) Cabeza, J. A.; del Río, I.; Riera, V.; García-Granda, S.; Sanni, B. *Organometallics* **1997**, *16*, 1743–1748.
 (53) Albinati, A.; Filippi, V.; Leoni, P.; Marchetti, L.; Pasquali, M.; Passarelli, V. *Chem. Commun.* **2005**, 2155–2157.
 (54) Carlton, L. *Bruker Rep.* **2000**, *148*, 28–29.

Table 7. Crystal Data and Structure Refinement for Complexes $[\text{NBu}_4]_2\{(\text{R}_F)_2\text{Pt}(\mu\text{-PPh}_2)_2\text{Pt}(\mu\text{-PPh}_2)_2\text{Pt}(\mu\text{-Cl})_2\} \cdot 5.5\text{Me}_2\text{CO}$ (**4**·5.5Me₂CO), $[\text{NBu}_4][(\text{R}_F)_2\text{Pt}(\mu\text{-PPh}_2)_2\text{Pt}(\mu\text{-PPh}_2)_2\text{Pt}(\text{acac})] \cdot 2\text{Me}_2\text{CO}$ (**5**·2Me₂CO), $[(\text{R}_F)_2\text{Pt}(\mu\text{-PPh}_2)_2\text{Pt}(\mu\text{-PPh}_2)_2\text{Pt}(\text{acac})][\text{ClO}_4] \cdot 3\text{CH}_2\text{Cl}_2$ (**6**·3CH₂Cl₂), $[(\text{PPh}_2\text{R}_F)(\text{R}_F)\text{Pt}(\mu\text{-PPh}_2)(\mu\text{-I})\text{Pt}(\mu\text{-PPh}_2)_2\text{Pt}(\text{PPh}_3)] \cdot 0.25\text{CH}_2\text{Cl}_2 \cdot 0.5n\text{-C}_6\text{H}_{14}$ (**9**·0.25CH₂Cl₂·0.5n-C₆H₁₄), and $[(\text{R}_F)_2\text{Pt}(\mu\text{-PPh}_2)_2\text{Pt}(\mu\text{-PPh}_2)_2\text{PtI}_2] \cdot 2\text{CH}_2\text{Cl}_2 \cdot 3\text{H}_2\text{O}$ (**11**·2CH₂Cl₂·3H₂O)

	4 ·5.5Me ₂ CO	5 ·2Me ₂ CO	6 ·3CH ₂ Cl ₂	9 ·0.25CH ₂ Cl ₂ ·0.5n-C ₆ H ₁₄	11 ·2CH ₂ Cl ₂ ·3H ₂ O
formula	C ₁₅₂ H ₁₄₆ Cl ₂ F ₂₀ N ₂ P ₈ Pt ₆ ·5.5Me ₂ CO	C ₈₁ H ₈₂ F ₁₀ NO ₂ P ₄ Pt ₃ ·2Me ₂ CO	C ₆₅ H ₄₇ ClF ₁₀ O ₆ P ₄ Pt ₃ ·3CH ₂ Cl ₂	C ₇₈ H ₅₅ F ₁₀ I ₂ P ₅ Pt ₃ ·0.25CH ₂ Cl ₂ ·0.5n-C ₆ H ₁₄	C ₆₀ H ₄₀ F ₁₀ I ₂ P ₄ Pt ₃ ·2CH ₂ Cl ₂ ·3H ₂ O
<i>M_r</i> [g mol ⁻¹]	4189.34	2117.79	2113.4	2236.93	2137.77
<i>T</i> [K]	100(1)	223(1)	100(1)	100(1)	100(1)
<i>λ</i> [Å]	0.71073	0.71073	0.71073	0.71073	0.71073
cryst syst	triclinic	monoclinic	monoclinic	triclinic	monoclinic
space group	<i>P</i> $\bar{1}$	<i>P</i> 2 ₁	<i>P</i> 2 ₁ / <i>c</i>	<i>P</i> $\bar{1}$	<i>C</i> 2/ <i>c</i>
<i>a</i> [Å]	13.042(2)	11.8212(4)	21.0543(9)	18.7253(7)	18.8343(14)
<i>b</i> [Å]	17.449(3)	20.0776(7)	10.8851(5)	20.8882(8)	26.2950(19)
<i>c</i> [Å]	8.659(3)	17.6024(6)	30.7207(14)	22.7255(8)	15.6164(12)
<i>α</i> [deg]	97.277(4)	90	90	90.644(1)	90
<i>β</i> [deg]	96.305(3)	95.251(1)	93.398(1)	109.611(1)	110.635(1)
<i>γ</i> [deg]	97.511(3)	90	90	97.570(1)	90
<i>V</i> [Å ³]	4140.9(12)	4160.2(2)	7028.1(5)	8285.6(5)	7237.8(9)
<i>Z</i>	1	2	4	4	4
<i>ρ</i> [g cm ⁻³]	1.680	1.691	1.997	1.793	1.962
<i>μ</i> [mm ⁻¹]	5.234	5.181	6.392	5.974	6.940
<i>F</i> (000)	2050	2080	4048	4240	4016
2 θ range [deg]	2.4–50.1	3.4–52.9	2.0–50.0	3.3–52.6	3.3–50.0
no. of reflns collected	22969	35852	37609	67365	19544
no. of unique reflns	14489	16574	12369	32989	6375
<i>R</i> (int)	0.0302	0.0417	0.0313	0.0502	0.0806
final <i>R</i> indices [<i>I</i> > 2 σ (<i>I</i>)] ^a					
<i>R</i> ₁	0.0455	0.0339	0.0262	0.0431	0.0697
<i>wR</i> ₂	0.1094	0.0560	0.0484	0.0891	0.1689
<i>R</i> indices (all data)					
<i>R</i> ₁	0.0707	0.0448	0.0333	0.0817	0.1119
<i>wR</i> ₂	0.1218	0.0580	0.0503	0.09495	0.1823
goodness-of-fit on <i>F</i> ^{2b}	1.014	0.817	1.036	0.995	1.052

$$^a R_1 = \sum(|F_o| - |F_c|) / \sum |F_o|. \quad ^b \text{Goodness-of-fit} = [\sum w(F_o^2 - F_c^2)^2 / \sum w(F_o^2)]^{1/2}. \quad \text{Goodness-of-fit} = [\sum w(F_o^2 - F_c^2)^2 / (n_{\text{obs}} - n_{\text{param}})]^{1/2}.$$

X-Ray Structure Determinations. Crystal data and other details of the structure analysis are collected in Table 7. Suitable crystals of **4**·5.5Me₂CO, **5**·2Me₂CO, **6**·3CH₂Cl₂, **9**·0.25CH₂Cl₂·0.5n-C₆H₁₄, and **11**·2CH₂Cl₂·3H₂O were obtained by the slow diffusion of *n*-hexane into an acetone (**4** and **5**) or CH₂Cl₂ (**6**, **9** and **11**) solution of the complex. Crystals were mounted at the end of a glass fiber. In all cases, the diffraction data were collected with a Bruker Smart Apex diffractometer. For **4**·5.5Me₂CO, unit cell dimensions were determined from the positions of 941 reflections from the main data set. For **5**·2Me₂CO, unit cell dimensions were determined from the positions of 9661 reflections from the main data set. For **6**·3CH₂Cl₂, unit cell dimensions were determined from the positions of 6921 reflections from the main data set. For **9**·0.25CH₂Cl₂·0.5n-C₆H₁₄, unit cell dimensions were determined from the positions of 8208 reflections from the main data set. For **11**·2CH₂Cl₂·3H₂O, unit cell dimensions were determined from the positions of 2489 reflections from the main data set. For all of the structures, the diffraction frames were integrated using the SAINT package⁵⁵ and corrected for absorption with SADABS.⁵⁶ Lorentz and polarization corrections were applied in all cases.

The structures were solved by Patterson and Fourier methods. All refinements were carried out using the program SHELXL-97.⁵⁷ All non-hydrogen atoms were assigned anisotropic displacement parameters and refined without positional constraints except as

noted. All hydrogen atoms were constrained to idealized geometries and assigned isotropic displacement parameters 1.2 times the *U*_{iso} value of their attached carbon atoms (1.5 times for methyl hydrogen atoms). For **4**·5.5Me₂CO, one of the Me₂CO solvent molecules was found to be disordered over two positions that were refined with 0.5 partial occupancy. The geometry in these disordered moieties was restrained to acceptable values, and all of the atoms were assigned a common set of anisotropic thermal parameters. For **9**·0.25CH₂Cl₂·0.5n-C₆H₁₄, two molecules of *n*-hexane and a molecule of dichloromethane were found and refined at 0.5 occupancy each, and, in the case of *n*-hexane, with isotropic displacement parameters. No H atoms were assigned to the solvent molecules. Full-matrix least-squares refinement of these models against *F*² converged to final residual indices given in Table 7.

Acknowledgment. This work was supported by the Spanish MCYT (DGI)/FEDER (Project CTQ2005-08606-C02-01) and the Gobierno de Aragón (Grupo de Excelencia: Química Inorgánica y de los Compuestos Organometálicos). S.I. acknowledges the Ministerio de Ciencia y Tecnología for a grant.

Supporting Information Available: Further details of the structure determinations of **4**·5.5Me₂CO, **5**·2Me₂CO, **6**·3CH₂Cl₂, **9**·0.25CH₂Cl₂·0.5n-C₆H₁₄, and **11**·2CH₂Cl₂·3H₂O including atomic coordinates, bond distances and angles, and thermal parameters and ¹⁹F HMQC; experimental and calculated ³¹P{¹H}, ¹⁹⁵Pt{¹H}, and ¹⁹F–³¹P HMQC; ¹⁹F–¹⁹⁵Pt HMQC; and ³¹P{¹H}-COSY spectra. This material is available free of charge via the Internet at <http://pubs.acs.org>.

IC8011124

(55) SAINT, version 5.0; Bruker Analytical X-ray Systems: Madison, WI.

(56) Sheldrick, G. M. SADABS; University of Gottingen: Gottingen, Germany, 1996.

(57) Sheldrick, G. M.; SHELXL-97; University of Gottingen: Gottingen, Germany, 1997.

(58) Formiés, J.; Fortuño, C.; Ibáñez, S.; Martín, A. *Inorg. Chem.* **2008**, *47*, 5978–5987.